

## REVIEW

[View Article Online](#)  
[View Journal](#) | [View Issue](#)



Cite this: *Nanoscale Adv.*, 2023, 5, 571

## Nanotechnology-based diagnostics and therapeutics in acute lymphoblastic leukemia: a systematic review of preclinical studies†

Reyhane Khademi, <sup>‡\*abc</sup> Zahra Mohammadi, <sup>de</sup> Rahele Khademi, <sup>ab</sup> Amene Saghazadeh <sup>fg</sup> and Nima Rezaei <sup>\*fgh</sup>

**Background:** Leukemia is a malignant disease that threatens human health and life. Nano-delivery systems improve drug solubility, bioavailability, and blood circulation time, and release drugs selectively at desired sites using targeting or sensing strategies. As drug carriers, they could improve therapeutic outcomes while reducing systemic toxicity. They have also shown promise in improving leukemia detection and diagnosis. The study aimed to assess the potential of nanotechnology-based diagnostics and therapeutics in preclinical human acute lymphoblastic leukemia (h-ALL). **Methods:** We performed a systematic search through April 2022. Articles written in English reporting the toxicity, efficacy, and safety of nanotechnology-based drugs (in the aspect of treatment) and specificity, limit of detection (LOD), or sensitivity (in the aspect of the detection field) in preclinical h-ALL were included. The study was performed according to PRISMA instructions. The methodological quality was assessed using the QualSyst tool. **Results:** A total of 63 original articles evaluating nanotechnology-based therapeutics and 35 original studies evaluating nanotechnology-based diagnostics were included in this review. As therapeutics in ALL, nanomaterials offer controlled release, targeting or sensing ligands, targeted gene therapy, photodynamic therapy and photothermic therapy, and reversal of multidrug-resistant ALL. A narrative synthesis of studies revealed that nanoparticles improve the ratio of efficacy to the toxicity of anti-leukemic drugs. They have also been developed as a vehicle for biomolecules (such as antibodies) that can help detect and monitor leukemic biomarkers. Therefore, nanomaterials can help with early diagnostics and personalized treatment of ALL. **Conclusion:** This review discussed nanotechnology-based preclinical strategies to achieve ALL diagnosis and therapy advancement. This involves modern drug delivery apparatuses and detection devices for prompt and targeted disease diagnostics. Nonetheless, we are yet in the experimental phase and investigational stage in the field of nanomedicine, with many features remained to be discovered as well as numerous problems to be solved.

Received 26th July 2022  
Accepted 19th December 2022  
DOI: 10.1039/d2na00483f  
[rsc.li/nanoscale-advances](http://rsc.li/nanoscale-advances)

## 1 Introduction

Acute lymphocytic leukemia (ALL) is a kind of leukemia that develops when lymphocytes in bone marrow (BM) proliferate abnormally.<sup>1–8</sup> It is divided into two types based on the cell of origin: B-ALL and T-ALL. There are four stages of the treatment

for ALL, which usually take two to three years: induction, consolidation, intensification, and long-term maintenance. Besides, routine CNS prophylaxis is proposed, and allogeneic hematopoietic stem cell transplantation (Allo-HSCT) stands as the standard consolidation treatment in high-risk patients with an available donor.<sup>7–11</sup> If not treated, the leukemic cells are

<sup>a</sup>Systematic Review and Meta-Analysis Expert Group (SRMEG), Universal Scientific Education and Research Network (USERN), Tehran, Iran. E-mail: khademi.1358@yahoo.com

<sup>b</sup>Immunology Board for Transplantation and Cell-Based Therapeutics (Immuno\_TACT), Universal Scientific Education and Research Network (USERN), Tehran, Iran

<sup>c</sup>Department of Medical Laboratory Sciences, School of Para-medicine, Ahvaz Jundishapur University of Medical Sciences, Ahvaz, Iran

<sup>d</sup>Radiological Technology Department of Actually Paramedical Sciences, Babol University of Medical Sciences, Babol, Iran

<sup>e</sup>Systematic Review and Meta-Analysis Expert Group (SRMEG), Universal Scientific Education and Research Network (USERN), Babol, Iran

<sup>f</sup>Research Center for Immunodeficiencies, Children's Medical Center, Tehran University of Medical Sciences, Dr Qarib St, Keshavarz Blvd, Tehran 14194, Iran. E-mail: rezaei\_nima@tums.ac.ir; Rezaei\_nima@yahoo.com; Fax: +98-21-6692-9235; Tel: +98-21-6692-9234

<sup>g</sup>Integrated Science Association (ISA), Universal Scientific Education and Research Network (USERN), Tehran, Iran

<sup>h</sup>Department of Immunology, School of Medicine, Tehran University of Medical Sciences, Tehran, Iran

† Electronic supplementary information (ESI) available. See DOI: <https://doi.org/10.1039/d2na00483f>

‡ These authors equally contributed to the manuscript.



distributed to the blood circulation system and subsequently to vital body organs. Moreover, liquid tumors, such as leukemia, cannot be surgically removed, unlike solid tumors.<sup>4</sup> Current treatment regimens face significant obstacles, including (i) the need to use a high amount of agents to guarantee their delivery to target cells, (ii) the requirement to combine numerous agents to boost therapeutic efficiency and diminish the multidrug resistance (MDR) process, and (iii) the destruction of healthy tissues and drastic toxicity.<sup>2-4,12-14</sup> It has been demonstrated that while standard therapy can eliminate the bulk of the disease cell population, several resistant leukemic stem cells (LSCs) remain alive, leading to chemoresistance and unfavorable side effects.<sup>1-4,15,16</sup> There is a high societal cost in terms of healthcare and the quality of life for patients from the start of treatment until unending relapse-dependent therapy.<sup>6</sup> As a result, finding and developing smart delivery methods that efficiently preserve and distribute therapeutic medications, improve targeting capabilities, and accomplish controlled release are critical to healing leukemia.<sup>2-4,17-19</sup>

Conventional detection methods show some restrictions, such as being costly, laborious, and time-consuming.<sup>20</sup> They require a set of elaborated devices while suffering from low sensitivity and need several processing phases, which makes them unfavourable for easy and fast medical monitoring or analysis.<sup>21</sup> Hence, due to the demand for the discovery of better diagnostics and treatment approaches with the highest possible specificity and efficiency and minor toxicity, researchers are trying to develop modern strategies.<sup>13</sup>

Nanotechnology has recently been developed as a delivery system. A system with a size of 1–1000 nm is referred to as a nanosystem. It first appeared in the medical area in the 1990s, giving rise to nanomedicine. Nanotechnologies can encapsulate and distribute hydrophobic compounds that are difficult to freely administrate and enhance their solubility and biocompatibility.<sup>2,19,22</sup> The materials used for nanosystems must be biocompatible, non-toxic, biodegradable, and sufficiently stable for *in vivo* administration.<sup>2,9,10,12,15,19,23,24</sup> Nanomaterials also become great micro-spectroscopic contrasting agents or labels for imaging<sup>9,15,19,25,26</sup> which helps in fast, specific, and sensitive diagnostics and is beneficial in the discovery of minimal residual diseases (MRDs) after treatment.<sup>27</sup> Their extremely large surface areas give them multifunctional capability to load several therapeutic drugs accompanied by other factors like stealth agents, targeting elements, triggering strategies, magnetic features, or imaging traits. The multifunctional trait of nano-delivery complexes has been more studied in developing theranostic (therapeutic + diagnostic) strategies for attacking cancer through encompassing a multitude of drug agents with imaging probes to monitor and scan the therapeutic agents distributed in the body.<sup>12,16,28-30</sup> Theranostics provides real-time evaluation of the growth or spoiling of cancer cells.<sup>28,29</sup> However, non-viral nanoparticle delivery methods are still in the experimental stage. Several issues are to be addressed, including side effects, controlled release, targeted therapy, and the possibility of combinatorial therapy.<sup>2-4,10,31</sup>

This study systematically evaluated preclinical human-ALL research to explain the potential benefits and limitations of

nanomaterial application and provide an overview of their diagnostic and therapeutic efficacy and possible toxicity *in vitro* and/or *in vivo*. To our knowledge, this is the first in-depth systematic review of the literature on the function of nano-systems in preclinical h-ALL.

## 2 Methods

This study followed PRISMA instructions.<sup>32</sup>

### 2.1. Data sources

Electronic databases were used to conduct the literature search (PubMed, Scopus, and ISI Web of Science). The search was conducted using a set of keywords relevant to nano-based materials and their use in treatment or detection applications. The database search had no time limit and occurred on April 15, 2022. ESI File 1† includes database search terms for each database.

### 2.2. Data sources

During the study selection, a two-stage method was followed. The review writers assessed the title, abstract, and keywords against the qualifying criteria in the first step. If the studies were eligible or doubted to be included, they were selected for the second stage of the review, *i.e.*, detailed review. In the second step, the full text of the articles was reviewed, and the review authors evaluated the studies if they satisfied the eligibility criteria. Any discrepancies between reviewers were handled following discussion and agreement.

### 2.3. Eligibility criteria

Studies were included if they met the following criteria: (1) were written in English with the full text available; (2) used human-ALL as the objective disease; (3) were studied *in vitro* by using cellular lines and/or *in vivo* by using animal models; (4) research papers offered at least one treatment plan and/or one detection plan in comparison to routine approaches. Review articles were excluded. Interventions directing therapeutic substances coupled with nanostructures were of interest.

### 2.4. Data items and quality assessment

We created a data extraction sheet that was pilot tested and optimized for gathering data for this review. The information obtained from each selected paper included: (1) *in vitro* and/or *in vivo* patterns used, comparing the free drug effects against their nano-conjugations; (2) theranostics results depicted in words of diagnostic/therapeutic plans used, and therapeutic efficiency gained (determined by cellular viability, tumor size/volume diminution or histological examinations); (3) toxicity effects (also determined by cellular viability, animal survival rate or animal weight variations, or histological examinations); (4) nanomaterials as diagnostic tools in monitoring leukemic cells (also determined by specificity, sensitivity or LOD).

The studies were selected by full-text evaluation. Then, two reviewers separately assessed them for methodological quality



based on criteria taken from the QualSyst tool for quantitative/qualitative research<sup>33</sup> to meet the prerequisites of the present systematic review (Table S1 ESI†). All selected studies covered the minimum threshold for inclusion.

## 2.5. Outcomes

The primary outcomes were those associated with therapeutic effects and diagnostic applications. Therapeutic efficacy *in vitro* is assessed using tumor cell IC<sub>50</sub>/viability or differentiation status and the extent of tumor growth regression. *In vivo*, the quality of mice life, survival rate, remission status, event-free survival (EFS), overall survival (OS), and relapse rate apply for treatment evaluation. Secondary outcomes included the toxicity, side effects, and safety of the proposed nanomaterial systems for therapeutic reasons. The LOD, sensitivity, and specificity were of interest for detection purposes.

## 3 Results

The PRISMA flow diagram displays the study selection process (Fig. 1). Of 2804 studies found from PubMed, Web of Science,

and Scopus, 242 were removed as duplicates, and 2562 were screened. According to defined exclusion criteria, 2410 studies were excluded through abstract/title screening. One hundred and fifty two studies for treatment and detection were considered for the full-text evaluation, and 54 studies were also excluded because of not satisfying the inclusion criteria, using other cell lines instead of humane ALL ( $n = 5$ ),<sup>34–38</sup> not being totally relevant to our objective, or lacking detailed and obvious data ( $n = 23$  for treatment;<sup>39–61</sup>  $n = 14$  for detection)<sup>20,62–74</sup> and not having full-text publications available ( $n = 12$ ).<sup>54,75–85</sup> Finally, 63 articles matched the inclusion criteria for the treatment section ( $n = 63$ ) and 35 articles for the detection section ( $n = 35$ ). Tables 1–6 summarize the characteristics and findings of the studies included.

## 4 Discussion

Although the study designs, interventions, and duplicated results differed substantially, our team tried to describe systematically the results of the included studies (organized in Tables 1–6). We also tried to discuss their correlations, and

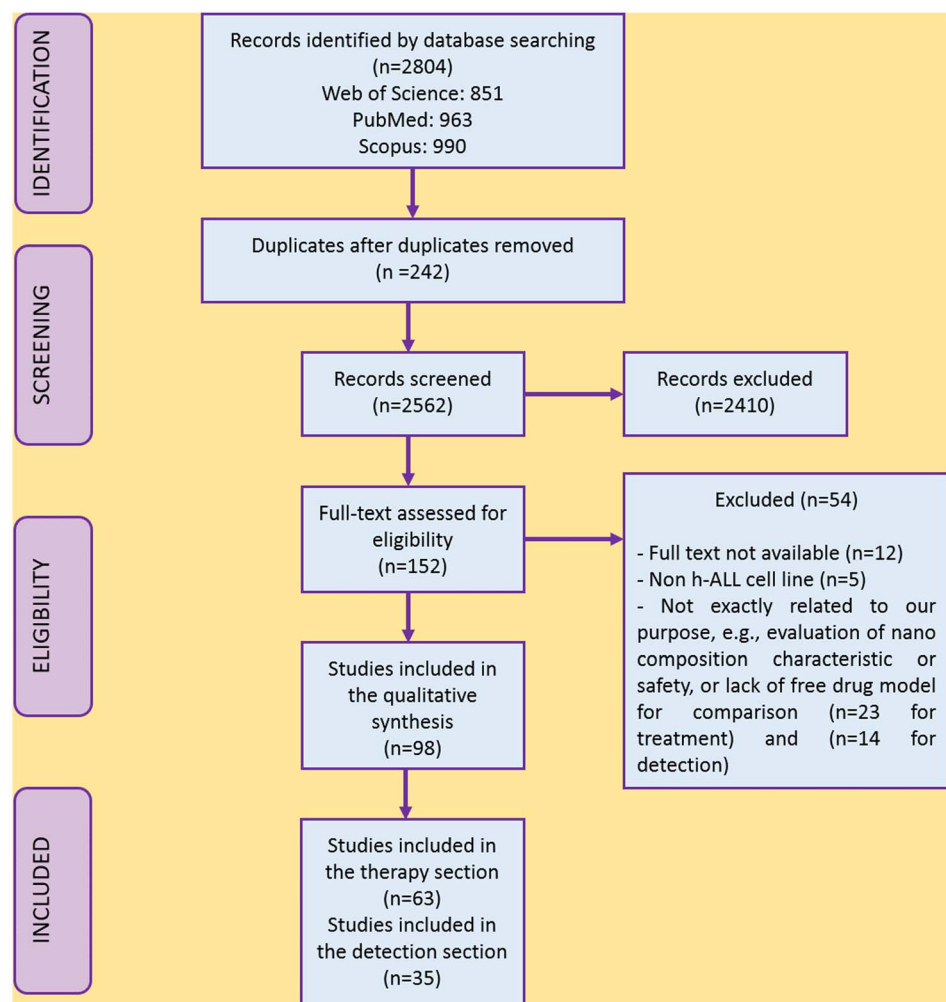


Fig. 1 PRISMA flow diagram of study selection.

Table 1 *In vitro* evaluation of triggers, sensing and control release of nano-drug complexes<sup>a</sup>

Cell line (year of study)	Nanomaterial/size	Drug, bioactive, gene, photosensitizer	Nano-drug efficacy on leukemic cells	Nano-drug cytotoxic effect on non-target/ healthy cells	Release status	Trigger
CCRF-CEM (2009) <sup>106</sup> Junkat (2011) <sup>22</sup>	DNA aptamer sg8c PEG-hydrophobic poly(β-amino ester) (PbAE)/ND	Doxorubicin (DOX) Paclitaxel/paclitaxel oleate in poly(ε-caprolactone) (PCL)	Similar to the free drug Similar to the free drug	Nontoxic ND <sup>a</sup>	(Acid-labile linkages) Controlled release (slow, sustained)	PH PH
CCRF-CEM (2017) <sup>108</sup>	sg8c-polyrotaxane-based nanoconstruct (PRNC), PEG/400 nm	Similar to the free drug	Nontoxic, Safer	Controlled release	PH	
CCRF-CEM (2018) <sup>109</sup>	Liposomal - PEG/110.37 nm	Vincristine (VCR)	Weaker cytotoxic than the free drug targeting form is similar to the free drug	Nontoxic, safer	Controlled release (sustained)	PH
6TC-CEM (T-ALL) (2018) <sup>105</sup>	Chitosan (CS), CSNP/ND	Zinc ion (Zn) antioxidant	More cytotoxic than the free drug	ND	ND	PH
Junkat (2021) <sup>111</sup>	PLGA/ND	Mercaptopurine (6 MP)	Weaker cytotoxic than the free drug	Nontoxic, safer	Burst release initiation, and PH then slow, sustained release	
Molt-4 (2011) <sup>107</sup>	sg8c-single-walled carbon nanotubes (SWNTs)/6 nm	Daunorubicin (Dau)	Similar to free drugs	Nontoxic, safer	Controlled release	PH
Molt-4 (2015) <sup>103</sup>	sg8c-AuNPs/15 nm	Daunorubicin (Dau)	More cytotoxic than the free drug	Nontoxic, safer	Controlled release	PH
Molt-4 (2016) <sup>104</sup>	sg8c-AuNPs/15 nm	Daunorubicin (Dau)	More cytotoxic than the free drug	Nontoxic, safer	Controlled release	PH
CCRF-CEM (2019) <sup>112</sup>	sg8c-MSN/103.24 nm	Doxorubicin (DOX)	Weaker cytotoxic than the free drug targeting form is similar to the free drug similar potent cancer cell killing with C14-4 LNPs, EP, or lentivirus	Nontoxic, safer	Controlled release (slow, sustained)	PH
Junkat cells co-culture assay with Nalm-6 (2020) <sup>110</sup>	Ionizable lipid nanoparticles (LNPs), C14-4/65.19 nm	CAR T cell: mRNA viral delivery, electroporation EP	Nontoxic, safer	Controlled release	PH	
CEM (2015) <sup>121</sup>	AgNPs-mesoporous silica nanospheres (MSNs) - PEG/90 nm	Paclitaxel (PTX)	Cytotoxic effect weaker than the free drug targeting form is similar to the free drug	Nontoxic, safer	Controlled release	GSH
CCRF-CEM (2019) <sup>120</sup>	Polymeric micelles (PCL-ss-Sg8c-BSA (polycaprolactone)) $165.1 \pm 5.2$ nm	Ara-C	Similar to the free drug targeting form is Nontoxic more cytotoxic than the free drug	Nontoxic, safer	Controlled release	GSH
CCRF-CEM (2011) <sup>115</sup>	sg8c-hp-Au NP/21.1 ± 1.6 nm	Doxorubicin (DOX)	Similar to the free drug	Nontoxic, safer	Controlled release	Light, temperature Irradiation
CCRF-CEM (2011) <sup>128</sup>	sg8c-G-quadruplex/ND	Photosensitizer TMPyP4 (porphine: parent of porphyrin)	More effective than TMPyP4 alone	Nontoxic, safer	ND	
Junkat (2016) <sup>100</sup>	poly(methyl methacrylate) (PMMA)/100 nm	Zinc(ii) phthalocyanine (ZnPc), (photosensitizer: PS)	More effective than free ZnPc	Nontoxic	Controlled release (slow, sustained), diffusion	Irradiation
CCRF-CEM LCK high (2020) <sup>129</sup>	DMAP-EDCI-DMF + zinc(ii) phthalocyanine (ZnPc), (photosensitizer: PS): C5/ND PEG-dipeptide linker-mAb/ND	Dasatinib (small-molecule tyrosine kinase inhibitor)	More cytotoxic than the free drug	ND	ND	Irradiation
Daudi cell (2002) <sup>14</sup>	Adriamycin (ADR)	Weaker cytotoxic than the free drug	Nontoxic	Controlled release (slow, sustained)	Enzyme	

<sup>a</sup> ND: not determined.

limitations, in a feasible qualitative evaluation as an alternative of a meta-analysis. The intention of this systematic review was to study the therapeutic, diagnosis and theranostic effects of various nanomaterials on human Acute Lymphoblastic Leukemia (h-ALL) pre-clinically. This systematic study was conducted since the NP system has not been analyzed in the aspect of either the therapy effect or diagnostics, and without this conception, the NP role in both the features is compromised.

#### 4.1. A brief overview of nanotechnology tools

It is worth to have a brief introduction of nanomaterials with their division in two main categories of organic and inorganic groups.

Organic nanoparticles (including PEG, liposomes, micelles, polysaccharides, proteins, and dendrimers) are usually biocompatible and biodegradable. Their high surface-to-volume ratio allows them to load many pharmaceuticals, while their surface chemistry and chemical features enable them to release the loaded molecule in a regulated control manner.<sup>15,86</sup> Pegylated nanoparticles (polyethylene glycol, PEG) may circulate in the bloodstream for a long time, namely as "stealth particles," since they can elude immune system detection and clearance.<sup>87,88</sup>

Liposomes are used as a drug delivery vehicle because of their unique ability to solubilize water-insoluble organic compounds, preserve pharmaceuticals from degradation, are straightforward to transport to the target location, and have low nonspecific toxicity. The liposome is kept in the circulation in typical healthy tissues because endothelial cells' tight connections prevent particles from leaking out of the channel.<sup>10,89</sup> Generally, with a hydrophilic PEG shell, polymeric micelles are an excellent drug delivery strategy for weakly water-soluble anticancer medicines. The polymeric micelles circulate in the blood for a long period and aggregate more at the tumor site, resulting in a more consistent drug release profile.<sup>10,89</sup>

Natural biopolymers include polysaccharides (chitosan) and protein nanoparticles like transferrin (TF) and albumin.<sup>90-92</sup> Human serum albumin (HSA) nanoparticles with free functional groups on their surfaces can be modified to increase complex stability or targeting ability.<sup>74,93</sup> Because tumor tissues have a faster metabolic rate and utilize HSA as a nutrient, significant amounts of HSA accumulation occur in cancer sites, making it an ideal carrier for anti-cancer medication delivery.<sup>12,94</sup> HSA's intrinsic autofluorescence is accompanied by several drug binding sites as a natural carrier of therapeutic molecules, making it a suitable biological theranostic agent.<sup>74</sup>

A dendrimer is a polymer nanocarrier with a spherical center and regular branches around it. Various generations of dendrimers were created by modifying the chemical groups on their surfaces (e.g., charge, basicity, and hydrogen bonding capability). Dendrimer-drug conjugates are also made by covalently connecting an antineoplastic agent to dendrimer's peripheral groups.<sup>89,91</sup> As a result, many drug molecules may be attached to each dendrimer molecule (multivalent), and the type of the connection bonds aids in the control of therapeutic molecule

release.<sup>89</sup> Multivalent interactions can overcome monovalent ones that are innately weak.<sup>95</sup> Another advantage of the dendrimer is attachment and assembling with DNA clusters (*i.e.*, DNA PAMAM).<sup>16,89</sup>

Inorganic nanoparticles have a wider range of size and composition-dependent physical characteristics, making them ideal for biological applications, including cell imaging and molecular detection. However, because they are less biocompatible, they are frequently mixed with organic materials for nano-safety. Many forms of inorganic nanoparticles, such as carbon nanotubes (CNTs), quantum dots, magnetic nanoparticles, silica-based, and noble metal nanoparticles (gold and silver, in particular), are employed in anti-cancer applications. These plasmonic-active nanoparticles with strong near-infrared (NIR) resonances can be effective light-to-heat converters for initiating hyperthermia inside living cells. Due to their high surface-to-volume ratio, they can also transport many different chemicals and pharmaceuticals for delivery applications.<sup>15,16,96,97</sup>

The construction, superficial area, mechanical rigidity, metallic properties, conductivity (both electrical and thermal), and ultra-light weight are some unique physical and chemical characteristics of CNTs. They display higher drug loading than standard liposomes and dendrimer drug carriers based on their large specific surface area. CNT-based medication delivery improves the solubility, blood circulation, and effective regulation of therapeutic release, resulting in lower doses and higher medicinal efficacy. They can be excreted from the body by the kidneys.<sup>15,89</sup>

Quantum dots (QDs), 2–10 nm semiconducting materials, were firstly introduced in 1980. Compared to traditional fluorescent immunolabelling, Ruan *et al.* found that QD-based immunolabelling had a more constant photo-intensity leading to significant time and cost savings. Moreover, QD signals have a more selective and brighter photostability than typical organic dyes. Multiplexed cancer biomarker imaging *in situ* on intact tumor tissue specimens for tumor pathology analysis at the histological and molecular levels is possible with QD-based nanotechnology. Compared to typical immunochemistry experiments, QD immunostaining has been more accurate in detecting low protein expression levels accompanied by a reduced background. QDs have the potential to replace untargeted drug delivery and thereby reduce chemotherapy's undesired effects.<sup>16,89,91</sup>

#### 4.2. Nanomaterials as therapeutics in ALL

Although the study designs differed substantially, we tried to systematically describe the included therapy related studies' results (Tables 1–3) and discuss their correlations and limitations in a qualitative manner.

**4.2.1. Controlled release.** Aside from protecting the medication agents from the outside milieu and successfully targeting the tumor location, the controlled release of the drug content of the nanosystem is one of the most important aspects of drug delivery approaches.<sup>15,17,98</sup> Because drug concentrations can fluctuate considerably between sub-therapeutic and hazardous



levels, this condition frequently leads to chemotherapy failure, necessitating continuous drug administration to the patient. In controlled-release delivery, on the other hand, the drug concentration does not fluctuate and has been found in concentrations that produce beneficial effects, even with reducing the amount of drug supplied<sup>99–101</sup> and consequently reducing side effects by maintaining a near-steady drug concentration at the intended leukemic cell.<sup>24</sup> Inadequate chemotherapeutic drug delivery to tumor tissue can result in tumor cell renewal and even the creation of resistant cells.<sup>102</sup> Drug content liberation from nanocarriers can be stimulated by certain microenvironmental parameters at the target location (e.g., pH changes<sup>22,103–113</sup> and enzymatic activities<sup>114</sup>) or by external stimuli (e.g., heat,<sup>115</sup> light,<sup>115</sup> electric and magnetic field or ultrasound)<sup>15,116</sup> (Fig. 2) as summarized in Table 1. The pH gradient between distinct cell compartments provides the basis for pH-mediated agent release at the cellular level. When nanoparticles enter cells by endocytosis and travel from the prime endosomes to the lysosomes (pH 4.5–5), the pH drops dramatically. Researchers have created a variety of pH-responsive nanosystems to apply acidic pH to control the drug release rates.<sup>15,59,117</sup> Indeed, numerous contacts (such as hydrogen bonds, electrostatic, covalent, noncovalent, hydrophobic, and  $\pi$ – $\pi$  stacking interactions) between nanoparticles and drug agents are utilized as triggering approaches for a pH-dependent liberation. Doxorubicin (DOX), the most often used medication displaying positive charges at physiological pH, favors an electrostatic interaction with negatively charged nanoparticles.<sup>106,118,119</sup> In the acidic milieu of the endosomal cavity, another study presented a triggering method by aptamer conjugation mediated with a pH labile linker.<sup>106</sup> Because Single Wall NanoTubes (SWNTs) have many delocalized  $\pi$  electrons, their external layers can be easily functionalized by  $\pi$ – $\pi$  interactions with drugs possessing a  $\pi$ -electron-rich structure like Daunorubicin (Dau). By protonation of  $-\text{NH}_2$  groups, acidic pHs improve hydrophilicity and increase drug solubility to be released from nanoparticles.<sup>107</sup> Only one study showed that 6-MP was more soluble in an alkaline environment than in an acidic one since the ester link of PLGA was easily dissolved under basic circumstances.<sup>111</sup>

and drug agents are utilized as triggering approaches for a pH-dependent liberation. Doxorubicin (DOX), the most often used medication displaying positive charges at physiological pH, favors an electrostatic interaction with negatively charged nanoparticles.<sup>106,118,119</sup> In the acidic milieu of the endosomal cavity, another study presented a triggering method by aptamer conjugation mediated with a pH labile linker.<sup>106</sup> Because Single Wall NanoTubes (SWNTs) have many delocalized  $\pi$  electrons, their external layers can be easily functionalized by  $\pi$ – $\pi$  interactions with drugs possessing a  $\pi$ -electron-rich structure like Daunorubicin (Dau). By protonation of  $-\text{NH}_2$  groups, acidic pHs improve hydrophilicity and increase drug solubility to be released from nanoparticles.<sup>107</sup> Only one study showed that 6-MP was more soluble in an alkaline environment than in an acidic one since the ester link of PLGA was easily dissolved under basic circumstances.<sup>111</sup>

It has been observed that many tumor cells overexpress certain proteases such as cathepsin and matrix metalloproteases. CALLA is an endoprotease known as NEP (E.C.3.4.24.11.) related to refractory ALL. Accordingly, a dipeptide linker was employed to conjugate adriamycin (ADM) to be cleaved selectively with the CALLA tumor-specific enzyme.<sup>114</sup> Chemically induced drug liberation, such as glutathione (GSH)-mediated release, is an ordinary strategy in drug delivery

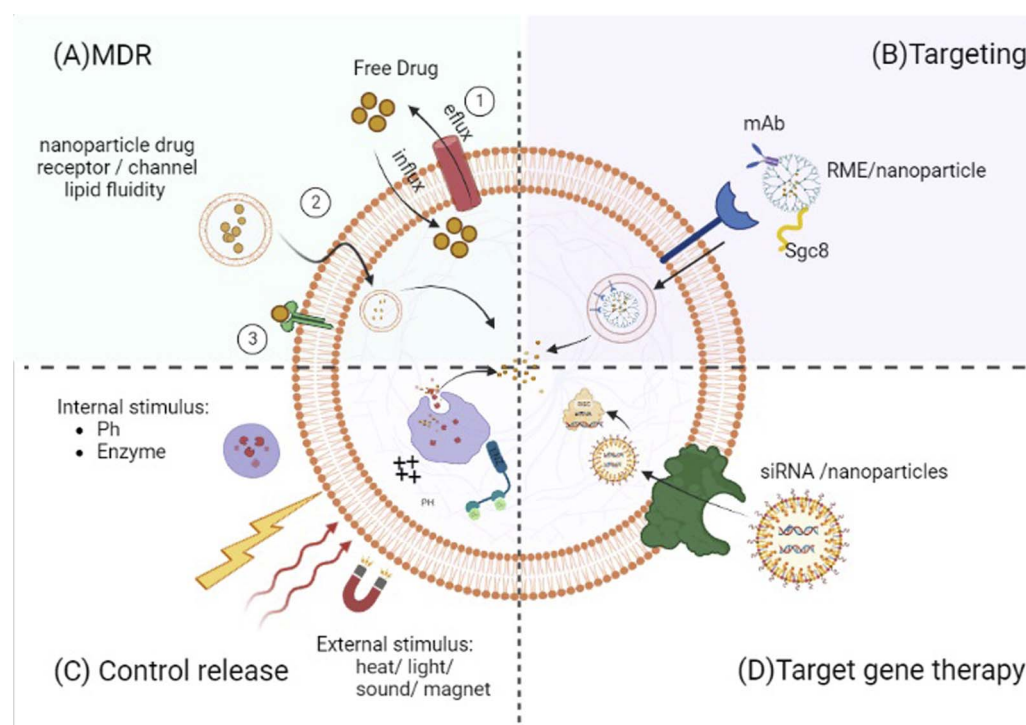


Fig. 2 Control release: drug content liberation from nanocarriers can be stimulated by certain microenvironmental parameters at the target location (e.g., pH change and enzymatic activities) or by external stimuli (e.g., heat, light, electric and magnetic field or ultrasound). Targeting: targeting ligands can specifically attach to the malignant cell (e.g., monoclonal antibodies (mAbs) or sgc8 aptamer). Targeted gene therapy: nanoparticle formation of targeted gene therapy agents (e.g., siRNA and TKIS) increased their anti-leukemic potency by enhancement of their stability and/or concentration. MDR (multi-drug resistance). Free small drugs move into malignant cells through passive transmission across the cell membrane, and they come into contact with membrane proteins such as drug efflux pumps leading to less than optimum amounts in the target cell. Lipid packing density and velocity can affect diffusion through the membrane. Increased membrane fluidity implies considerable drug permeability by delivering therapeutic agents into cancer cells without relying on specific receptors or channels, and nanoparticles can circumvent this resistance mechanism.

because of significant intracellular and extracellular variation of GSH amounts in some tumor cells. GSH can break disulfide bonds between drugs and nanocarriers and permit them to be released.<sup>15,120,121</sup>

Release methods dependent on particular changes in the surrounding media, such as pH, may, on the other hand, result in unpredicted distribution of payloads to different cellular sites and cell types. Developing a finely responsive system that is sensitive to minor environmental changes remains a key issue. As a result, far-away triggers that can be regulated exogenously come into the scene.<sup>115</sup> For example, a heat-dependent drug liberation can be designed in the nanosystem coupled with a temperature-sensitive polymer.<sup>15</sup> The temperature-dependent laser light causes the slow release of Dox molecules from the nanocarrier hp-AuNP by the input photon energy leading to a local photothermal heating reaction (hyperthermia).<sup>115</sup>

Several nanoparticles that selectively and serially react to two or more stimuli have been created to increase controlled drug release. Various combinations of stimuli were tested with activation by synchronous triggers in one cellular area or in a serial manner as the particle moves through different biological sections. These strategies resulted in greater drug release, which promised curative efficiency improvement.<sup>15,59,115</sup>

Last but not least, it is worth mentioning that drug diffusion,<sup>100,102,122</sup> solvent,<sup>122,123</sup> degradation, erosion,<sup>99</sup> swelling, and selective burst,<sup>74,111,120</sup> in addition to stimuli-controlled release are some strategies of drug release from nanocarriers. As more water enters the nanocapsules, water–polymer interactions become more likely than polymer–polymer interactions, causing the separation of polymer chains and disassembly of the nanoparticle in the erosion release profile.<sup>99</sup> The slow and sustained release of the drug encapsulated within the stable

core of serum albumin nanoparticles may be preceded by a fast initial burst release or erosion due to the breaking of the surface-adsorbed drug.<sup>74</sup> The PEG section also plays a key role in controlling the drug release rate that ensures prolonged release, which may cause drug diffusion and dissolution from the reservoir to be slow and sustained.<sup>24,109</sup> Generally, the quick release is thought to aid in achieving effective blood concentrations and promoting immediate illness alleviation, while the sustained release aids in maintaining a stable blood concentration. As a result, a lengthy exposure duration maintains significantly larger agent concentrations in the cells, resulting in more damage and increased cell death.<sup>111</sup>

**4.2.2. Targeting or sensing ligands.** Various types of nanogates permit the liberation of loaded drug agents into a peculiar milieu in reaction to different stimuli. Some stimuli can be operated in both tumor and normal cells because of little variations. In this case, targeting or sensing ligands are helpful. They can precisely attach to malignant cell overexpressed receptors (Fig. 2). Therefore, the uptake of normal cells or off-target destruction diminishes.<sup>6,12,15,16,121,124,125</sup> All of the targeting tactics applied in the literature reviewed have been presented in Table 2. A higher chemotherapeutic drug concentration, longer exposure duration, and ultimately enhanced cytotoxicity arise from high absorption of the targeted particles by leukemia cells.<sup>103,104,113,126</sup> Total body irradiation (TBI) has been routinely performed in pre-transplant management since the 1960s to treat leukemia because of its success and ability to penetrate too deeply into sanctuary sites. However, the utmost limit of this technique is toxicity to non-target tissues.<sup>127</sup> The release of the photosensitizer from specifically targeted nanoparticles also produced high toxicity

Table 2 List of targeting factors used to functionalize nano-conjugated drugs and direct them to leukemia cells<sup>a</sup>

Ligand/nano-drug target	Function	Internalization mechanism
Anisamide (AA) <sup>126</sup>	Targets overexpressed sigma receptors	ND
Sgc8 <sup>(94, 103, 104, 106–109, 112, 113, 115, 118–121, 128, 141 and 194)</sup>	Targets PTK7 (protein tyrosine kinase-7) overexpressed in T-ALL cells	Internalized <i>via</i> endocytosis
Anti-CD19(Ab) <sup>131,133,195</sup>	Targets CD19 overexpressed in B-ALL cells	Internalized <i>via</i> endocytosis
NL1 antibody <sup>114</sup>	Targets overexpressed CALLA (CD10) in B-ALL cells	Internalized <i>via</i> endocytosis
Anti-CD3e f(ab')2 fragments <sup>132</sup>	Targets CD3 on T-cells	Internalized <i>via</i> endocytosis
Heptapeptide DT7, transferrin <sup>90,136</sup>	Targets the transferrin receptor (TfR, also named CD71) overexpressed in T-ALL cells	Internalized <i>via</i> endocytosis
Peptidomimetic LLP2A <sup>125</sup>	Targets activated $\alpha 4\beta 1$ integrin expressed on childhood ALL cells	Internalized <i>via</i> endocytosis
Nonapeptide CD21 (CR2) <sup>135</sup>	Targets CD21 (CR2)	Internalized <i>via</i> endocytosis, pinocytosis
CD22 $\Delta$ E12 SiRNA <sup>50,146</sup>	Targets CD22 $\Delta$ E12 in aggressive B-ALL cells	None
WHI-P131 (ref. 87)	Targets tyrosine kinase JAK3 that regulates the activation of some important oncogenic proteins	None
C61 (ref. 145 and 146)	Targets the SYK inhibitor in the resistance B-ALL cells	None
Dasatinib <sup>129</sup>	Targets LCK tyrosine kinase	None
Amino acid L-Phe <sup>150</sup>	Targets Pyruvate kinase, PK, to reduce the ROS level	None

<sup>a</sup> ND: not determined.



to target cells along with little toxicity to non-target cells that faced irradiation light.<sup>115,128-130</sup>

Several chemical techniques for targeting the functionalization of nanomaterials with particular monoclonal antibodies (mAbs) for specific recognition of cell-surface proteins have been discussed.<sup>114,131-134</sup> Pendant-type immunoliposomes covered with a mAb demonstrate a greater internalization efficiency than immunoliposomes with antibodies covalently attached to the nanosystems.<sup>131</sup> Small benzamides, such as anisamide (AA), can also target overexpressed sigma receptors in various human cancer cell types.<sup>126</sup> Due to the upregulation of receptors on the surface of cancer cells, targeted nanoparticles can discriminate between cancer and normal cells.<sup>95</sup> In this review, we can point to some peptidomimetic ligands with high affinity and high specificity like LLP2A against activated  $\alpha 4\beta 1$  integrin,<sup>125</sup> a nonapeptide for CD21 (CR2),<sup>135</sup> and heptapeptide DT7, as a new target for the transferrin receptor (TFR or CD71 which is highly expressed in T-ALL cell lines).<sup>136</sup>

Because ALL is a liquid tumor, passive targeting through the increased permeability and retention (EPR) effect is not applicable. The gathering of non-targeted nanoparticles in the liver and spleen can be beneficial in the treatment of ALL, which are the main organs for leukemic blast accumulation and proliferation. In contrast, nanoparticle accumulation reduces its active filtration or clearance by organs like lungs and kidneys.<sup>17</sup> The biology and cytotoxicity effects of nanoparticles are governed by their physicochemical qualities. For example, the charge of the nanostructure has been linked to the interactions with various cellular characteristics or receptors and causes distinct results in target cells. Thus, nanostructures prefer cancer cells to PBMCs (despite sharing the same origin with leukemic cells).<sup>105,137,138</sup> However, the absence of targeting ligands restricts the uptake rate of leukemic cells, mostly *in vivo*, regardless of their existence in the systemic circulation flow.<sup>17</sup> The IC<sub>50</sub> values of some drug-conjugated nanoparticles of therapeutic agents were similar to or higher than those of the free drug in some studies.<sup>17,94,102,108,109,111,119,120,122,123,128,131,134</sup> A possible explanation is that the special receptor for conventional drugs (e.g., multidrug and toxin extrusion protein 1, MATE1, accepting imatinib as a substrate) is not available within the nanosystem formulation.<sup>139</sup> Furthermore, the drug-nanoparticle complex may represent a negatively charged nanomaterial similar to the charge of the cell membrane, and consequently, it is impossible to be taken up *via* passive processes. Thus, without targeting the nanoparticles, the drug uptake and efficacy may be diminished.<sup>119</sup> Finally, even in targeted-nanoparticle ones, the nanoparticle must first be internalized *via* endocytosis or phagocytosis and then released into the space.<sup>102,111,115,140</sup> In contrast to the time delay for cellular uptake and release of drugs from nanosystems, free drugs diffuse immediately. IC<sub>50</sub> values are influenced by the drug toxicity and the cell viability, as the termination point. A time delay for cytotoxicity induction is an important item in accepting the absence of significant differences in the IC<sub>50</sub> values between free and encapsulated forms.<sup>17,74</sup> The internalization mechanisms of nanoparticles include macrophagocytosis,<sup>135</sup> caveolin,<sup>119</sup> and clathrin-dependent<sup>15</sup>

endocytosis.<sup>133</sup> Targeting agents usually enter cells *via* receptor-mediated endocytosis (RME).<sup>107,118,136</sup>

It has been shown that targeted drug delivery may not significantly change the cell viability or drug's intracellular concentration compared to the drug alone. In contrast, high toxicity and intracellular drug concentration were seen in the drug-targeted-nanoparticle complex.<sup>107</sup> It can be explained by the fact that the large surface area of nanoparticles offers the possibility of the presence of multiple building blocks of the targeting ligand.<sup>104</sup>

The Sgc8 aptamer is the most commonly used targeting ligand in the studies evaluated in this review. It binds specifically to PTK7, a transmembrane receptor protein tyrosine kinase and a potential biomarker for T-ALL.<sup>94,103,104,106-109,112,113,115,118-121,128,141,142</sup> Moreover, PTK7 knockdown suppresses the Wnt signaling pathway, affecting cell proliferation and tumorigenesis.<sup>142</sup> The more stability of aptamers rather than antibodies makes them suitable for difficult conditions such as high temperatures.<sup>143</sup> Moreover, aptamers have a smaller size relative to antibodies, leading to more and faster penetration into cancer tissues.<sup>94</sup> Some studies used aptamers as both drug delivery carriers and targeting ligands.<sup>103,104,106,141</sup> However, besides the high cost, it is necessary to point to its renal filtration and nuclease degradation in the biological environment. Researchers are trying to make modifications to further improve aptamers' properties, like conjugating them to nanoparticles.<sup>1,103,104,142</sup> Besides, a high salt concentration in biological liquids could aggregate nanoparticles (e.g., AuNPs or SWNTs). Conjugation with an aptamer could enhance the solubility of nanoparticles and prevent them from aggregation.<sup>103,104</sup> A poly-aptamer-drug complex as a polyvalent aptamer complex displayed noticeably more efficiency than its monovalent analog in both cytotoxicity and selectivity as opposed to leukemia cells because of the amplified binding affinity of multivalence.<sup>94,103,118,142</sup> The feasibility of incorporation of multiple drug molecules within one aptamer was assumed. Although this operation is relatively impossible in the usual mAb-based immunoconjugate methodology, the IC<sub>50</sub> of sgc8c-3Dox compared to that of sgc8c-Dox with target cells showed no significant difference, which was less than expectations. This phenomenon was attributed to the reduced binding space and, as a result, the ability of the aptamer in the form of sgc8c-3Dox to bind to target cells.<sup>106</sup>

Most nanoparticle formulations decorated with target agents enhanced the anti-leukemic effect *in vitro* and *in vivo* more than typical drug solutions. Leukemic mice that underwent the treatment of drug-targeted-nanoparticles lived longer and exhibited lower obvious systemic toxicity than mice treated with traditional free therapeutic agents.<sup>108,109,120,121,133</sup>

An ideal and most favorable nanoparticle system would put together the high stability level of drugs with high loading proportions to reduce the amount of the drug content essential for administration and improve the selectivity for target tissue sites.<sup>124</sup> Some studies showed that drugs nanoencapsulated without targeting ligands have more potent anti-leukemic activities than free ones. The nanomaterials utilized included dendrimers,<sup>100,138</sup> chitosan (CS),<sup>99,105</sup> human serum albumin



nanoparticles (HSA),<sup>94</sup> liposomes,<sup>126</sup> and polymer PLGA-PEG.<sup>144</sup> The following factors can explain the improved efficacy of nanoencapsulation: (i) a high rate of metabolism in tumor cells and, as a result, higher consumption of nanomaterials (e.g., HSA) as a source of energy,<sup>94</sup> (ii) protection of agents attached from enzymatic degradation in biological media,<sup>92,126,138</sup> and (iii) improved uptake, better internalization properties, control, and sustained release mediated by nano-encapsulation.<sup>99,100,105,122,126,144</sup> Poor aqueous solubility limits the hydrophobic chemotherapeutic drugs' utility, leading to accumulation and aggregation in biologic environments. Biomaterial-based strategies can address this problem and help as drug delivery apparatus by increasing drug uptake.<sup>74,99,100,122,138,144</sup> Cationic nanoformulations interact strongly with negatively charged cell membrane surfaces for immediate internalization.<sup>105,126,138</sup>

Albumin-bound molecules aggregate preferentially in tumors due to the secretion of the albumin-binding SPARC (secreted protein, acidic, and rich in cysteine) protein. The reduced apoptosis of cells might, on the other hand, be due to albumin's well-known anti-apoptotic actions.<sup>74</sup>

Instead of passive diffusion of the medication across the membrane, encapsulating the drug in liposomes permits it to be delivered into the cells' interior by vascular fusion with the membrane.<sup>90</sup> The trafficking channels and amounts of enzymes for cleaving drugs from their carrier differ in leukemic and normal cells. The conjugate's cellular accumulation depends on the drug influx and efflux activities. Free drugs were usually transported quicker to leukemic cells than their conjugate. Additionally, the rate of drug-conjugated efflux in leukemia cells was lower than in free ones, while they were equivalent in normal PBMC.<sup>90</sup>

**4.2.3. Targeted gene therapy.** Targeted therapy is a type of treatment that works by disrupting the main molecules that cause leukemia. The primary treatment strategies are small molecule inhibitors that target gene mutations and key signaling pathways and antibodies or antibody-medicine conjugates that target cell surface molecules. Non-hematological side effects and drug resistance mechanisms may result in a decrease in the clinical therapeutic efficacy and application. However, nanoparticles specifically loaded with antibody medications improve leukemia cell killing efficacy, have higher specificity than regular antibody therapies, and considerably reduce leukemia recurrence.<sup>4</sup> This review included seven studies involving different target therapies that used Liposomal NanoFormulation<sup>50,87,110,131,132,145,146</sup> and demonstrated that nanoparticle formation significantly increased their anti-leukemic potency *in vitro* and in animal models without adding serious unwanted toxicity, as discussed below (Fig. 2).

Although high-dose imatinib, a BCR-ABL tyrosine kinase inhibitor, was recommended to overcome imatinib resistance, it had to be stopped due to toxicity. The IC<sub>50</sub> of imatinib-PEG-liposomes (liposomal nanoparticles (LNPs)) was greater than that of free imatinib, which can be explained by the nanomaterial covering the particular receptor, MATE1. Imatinib-CD19-PEG-liposomes had stronger anti-leukemic effects, with less damage to normal hematopoietic progenitor cells than free

imatinib, and prevented the development of cobblestone areas (CAs) of leukemia cells from patients with imatinib resistance.<sup>131</sup>

WHI-P131-NP, a nanoencapsulated tyrosine kinase JAK3 inhibitor, outperformed WHI-P131 and vincristine *in vivo*, regardless of chemosensitivity or resistance profile.<sup>87</sup>

Besides the damage to non-hematopoietic organs as a key restriction,<sup>127</sup> TBI-based therapy regimens cannot prevent leukemic relapses after HSCT, especially in high-risk cases with radiation-resistant BPL cells. The invention of novel drugs that can dominate the radiation resistance BPL cells would be a great step in attempts to improve post-HSCT results.<sup>146</sup> Spleen tyrosine kinase (SYK) is a chief regulator of anti-apoptotic signaling pathways in B-ALL cells. Compound 61 (C61), as a highly selective SYK inhibitor, induces apoptosis in the resistance malignant B-ALL cells. C61's low water solubility and life-threatening off-target adverse effects, on the other hand, have proven to be substantial roadblocks to its continued development as an anti-leukemic therapeutic candidate. The anti-leukemic potency of C61-LNP 25A, a safe liposomal nanoparticle formulation, was much higher than irradiation against aggressive radiation-resistant B-precursor ALL. Because irradiation/chemotherapeutic-resistant leukemic cells do not have cross-resistance to C61, novel combination strategies with multiple chemotherapy agents can be explored.<sup>145</sup> Furthermore, the C61-LNP + TBI combination was outstandingly more efficient than either TBI alone or C61-LNP alone without causing significant adverse effects.<sup>146</sup>

Dysfunctional CD22 following deletion of exon 12 (CD22ΔE12) represents aggressive B-ALL cells. The mutant protein is deficient in most intracellular domains considered the key regulatory signal transduction items.<sup>46</sup> The expression of genes correlated with the MAPK, PI3-K/mTOR, and WNT pathways was elevated differently in response to CD22ΔE12.<sup>51</sup> Leukemia gene therapy by small interfering RNA (siRNA) (an effector of the RNA interfering pathway that may down-regulate specific genes linked to disease pathology) has shown considerable promise in leukemia treatment.<sup>46</sup> Due to fast enzymatic breakdown in the blood, fast clearance rate, and poor entrance rate into target cells, systemically given unformulated siRNA has little RNAi action *in vivo*.<sup>6,50</sup> Genes and short RNAs can be electrostatically linked to nanoparticles or conjugated onto their surfaces. Natural organic polymeric nanoparticles, synthetic polymers, and inorganic nanoparticles (including carbon nanotubes, gold nanoparticles, and quantum dots<sup>44</sup>) have all been extensively exploited as cancer gene carriers in numerous cancer treatment studies.<sup>89</sup> Nanocarriers in gene therapy should have three critical characteristics: high loading efficiency, the ability to be carried from endosomes to the cytosol, and the ability to release the genetic material.<sup>110,147</sup> Using lipid nanoformulations (LNPs) of CD22ΔE12-siRNA, both CD22ΔE12-radiation and -chemotherapy-resistant leukemic clones were killed. A CD22ΔE12-siRNA LNP, alone or combined with chemotherapeutic medicines, was much more effective than those treatments alone in preventing leukemic clonogenicity *in vitro* and *in vivo*.<sup>50</sup>



Current high-cost clinical-scale T lymphocyte production (for chimeric antigen receptors, CAR-T cell) necessitates a series of complex methods, including extracting, genetically altering, and selectively expanding the genetically engineered T cells before re-injecting them into the patient.<sup>6,110,132</sup> These present CAR T cell engineering strategies rely on viral delivery, which results in persistent CAR expression and the danger of severe consequences associated with viral transduction. Although mRNA has been introduced as a possible technique for producing transitory CAR expression in T cells without causing genomic changes and mitigating the negative consequences of viral expression, it is most typically used in electroporation (EP) for T cell transfection, which can be cytotoxic. Using C14-4 ionizable lipid nanoparticles (LNPs), Billingsley *et al.* effectively transferred CD19-targeted CAR mRNA to primary human T cells with the same powerful cancer cell killing of EP or lentivirus CAR-T cells generated while reducing cytotoxicity related to EP.<sup>110</sup> In another study, nanoparticles containing CD19-specific CAR genes were shown to alter T-cell specificity *in vivo* as they circulated, resulting in leukemia regression with success comparable to standard adoptive transfer of laboratory-made CAR T-cells (*via* lentivirus) while avoiding its complications.<sup>132</sup>

The overexpression of nucleophosmin (NPM) has also been linked to the development of multidrug resistance (MDR) in ALL, prompting the creation of a synthetically produced recombinant NPM binding protein (NPMBP).<sup>148,149</sup> Despite having degradable free NPMBP, the DOX-PMs-NPMBP nanoparticles dramatically reduce leukemia cell proliferation, cause apoptosis, and increase the anti-leukemia effect in resistant ALL cells *in vitro* and *in vivo*.<sup>148</sup>

A series of L-phenylalanine-based polymers (ester amide) (Phe-PEA), particularly Metabolic Reprogramming Immuno-surveillance Activation Nanomedicine (MRIAN), showed specificity-enhanced BM accumulation and crossing of the brain-blood barrier. It could enhance uptake by T-ALL and myeloid-derived suppressor cells (MDSCs) as an efficient delivery approach while sparing non-leukemic normal cells and reducing tissue toxicity. Accordingly, free Dox and even liposome-encapsulated Dox demonstrated lower cellular absorption rates than MRIAN-Dox-PLGA NP (Doxil). Besides the role of a drug carrier, it disturbed the immunosuppressive function of MDSCs by degradation to L-Phe amino acid.<sup>150</sup>

**4.2.4. Photodynamic therapy and photothermic therapy.** Non-invasive photodynamic therapy (PDT) for leukemia treatment has recently been established. PDT can efficiently filter

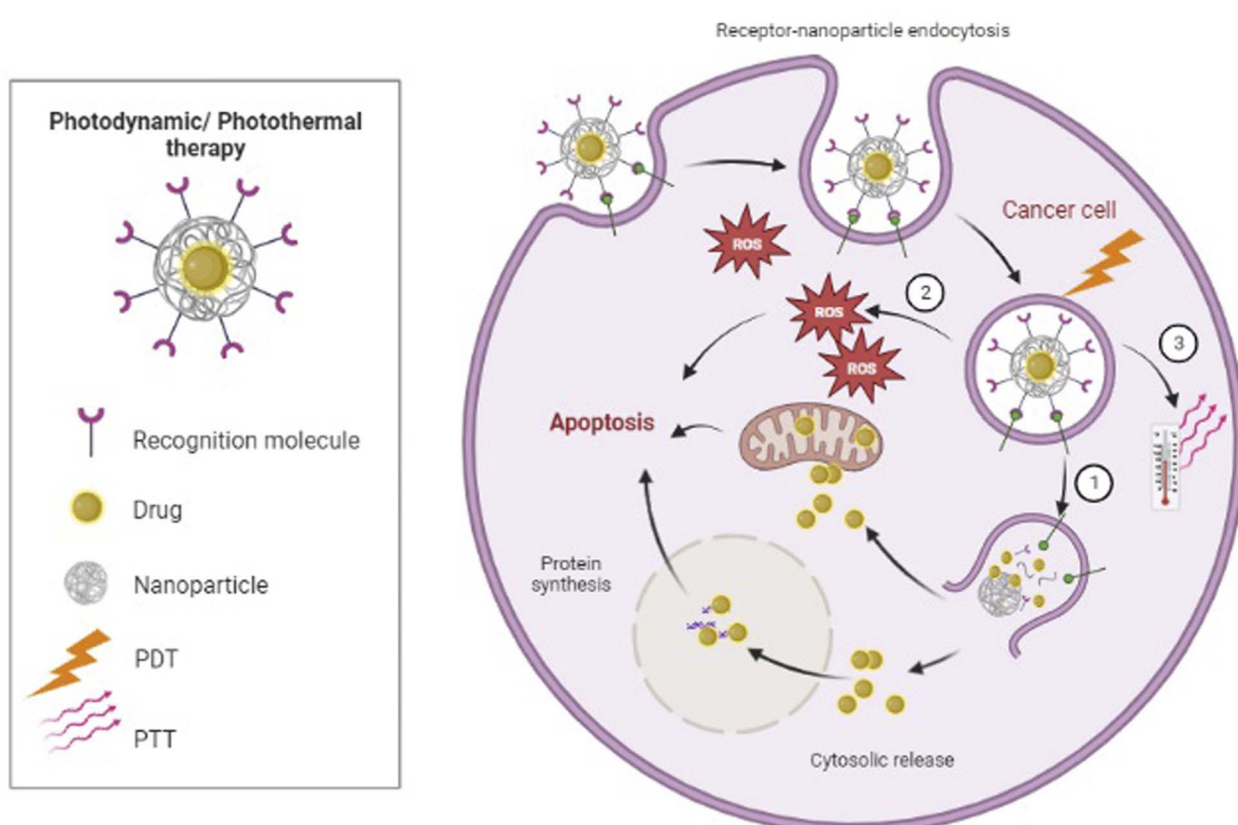


**Fig. 3** Photodynamic therapy (PDT): ① the irradiation light would be utilized for the release of the drug encapsulated. ② The irradiation light excite the photosensitizer (PS) in the tumor tissue, causing the PS to form a ROS that kills tumor cells. Photothermal therapy (PTT): ③ upon radiation absorption, CNTs or metal nanoparticles can transform photon energy to thermal energy, which results in a temperature rise and subsequently makes cellular destruction.



residual leukemia cells and limit leukemia recurrence, especially following autologous bone marrow transplantation.<sup>4</sup> PDT, in comparison to standard chemotherapy and radiation, is more target-specific, has fewer side effects, and has lower drug resistance. Three components are required: photosensitizer (PS), light, and oxygen (Fig. 3). In this process, the concentration of the PS in tumor tissue is greater than in surrounding normal tissues after a particular amount of time. The wavelength would then be utilized to excite the PS in the tumor tissue, causing the PS to form a ROS that kills tumor cells.<sup>4,151–154</sup> Due to low water solubility, poor photostability, and an extended retention period in the body, resulting in terrible skin photosensitivity and tissue harm, clinical usage of most PS is limited.<sup>129,151,152</sup> The non-aggregation of the PS in a biological medium and the PS's cellular absorption mechanism are critical for photobiological activity and phototoxicity. The free PS is absorbed *via* diffusion through the plasmatic membrane (lipophilic), which results in a low intracellular concentration in an aqueous solution.<sup>100</sup> Lipophilic zinc(II) phthalocyanine (ZnPc) and PS porphine ((tmpyp4), parent of porphyrin) as commonly used nontoxic photosensitizers are included for PDT in the studies included.<sup>100,128,129</sup> The therapeutic efficacy of PDT by the encapsulated PS in nanosystems is higher than in free PSs because the drug delivery nanosystems tend to prevent aggregation. ZnPc-loaded PMMA nanoparticles can also be administered without worrying about the undesired toxicity outcome on human blood cells.<sup>100</sup> Targeting the G-quadruplex-Sgc8 aptamer transfer of tmpyp4 PS provided higher phototoxicity to target cells with the advantages of decreases in toxicity to non-target cells, needed PS concentration, incubation time, and irradiation energy.<sup>128</sup> The presence of leukemia throughout the body complicates the proper light delivery required for PDT. Although these studies indicate that PDT can be used to cure leukemia *in vitro*, they do not prove that PDT can be used to treat leukemic cells *in vivo*.<sup>151,152</sup> Novel compound 4 (C4), which contains dasatinib as the targeting and zinc(II) phthalocyanine as the photodynamic moiety, has a strong affinity for CCRF-CEM cells, which overexpress lymphocyte-specific protein tyrosine kinase (LCK), as well as good photocytotoxicity for tumor regression. Significantly, PDT can boost immune responses in nude mice with CCRF-CEM tumors, perhaps leading to secondary cancer cell death and systemic anticancer immunity.<sup>129</sup>

Non-invasive photothermal therapy (PTT) is another nanoparticle-based therapeutic strategy. Upon radiation absorption, CNTs or metal nanoparticles such as Au-based nanomaterials can transform photon energy to thermal energy, which results in a temperature rise and subsequently causes cellular destruction or death due to hyperthermia<sup>155,156</sup> (Fig. 3). Nonetheless, PTT as a single therapy is generally not enough for complete tumor ablation.<sup>155</sup> Wang *et al.* designed a model of multimodal therapy, PDT accompanied by PTT, for attacking and destroying T-ALL, but their study did not fit our inclusion criteria. However, they demonstrated that PTT/PDT had a synergistic effect and could kill more tumor cells than either therapeutic strategy alone.<sup>156</sup>

**4.2.5. Nanotechnology for the reversal of multidrug-resistant ALL.** Different microenvironmental and cellular events can lead to acquired stability or resistance to one or more (chemo)-therapeutic agents (MDR, Multi-Drug Resistance). The cell survival pathways, inability to apoptosis induction, and overexpression of peculiar membrane-set drug efflux pumps (e.g., P-glycoproteins) are some processes of this cellular phenomenon.<sup>10,93,148</sup>

By altering the pharmacokinetic features of therapeutic agents, nanomedicines will raise the probability of active chemicals showing increased circulatory retention and local concentrations at the place of interest but, at minimum, exposed to healthy organs.<sup>10,50,87,145,146,148,157,158</sup> Accordingly, nanomedicines may somewhat, if not fully, overcome MDR. Because free small drugs almost entirely move into malignant cells through passive transmission across the cell membrane, they contact membrane proteins such as drug efflux pumps leading to less than optimum amounts in the target cell, resulting in MDR<sup>10</sup> (Fig. 2). Nanomedicines are still frequently taken up through endocytosis,<sup>10,133</sup> so receptor-mediated endocytosis is considered for 100–200 nm nanoparticles, whereas phagocytosis is used for bigger (500 nm) and smaller (25 and 50 nm) ones.<sup>101</sup> As a result, they skip the drug efflux mechanism, resulting in a significantly higher concentration within the cell than with a free drug.<sup>10</sup> Some anti-leukemic drugs, such as cisplatin and doxorubicin, have induced apoptosis in tumor cells *via* increasing cell membrane fluidity and clustering of lipid rafts.<sup>52</sup> The lipid packing density and velocity can affect diffusion through the membrane. Increased membrane fluidity implies considerable drug permeability. Cholesterol, which is known to diminish the fluidity of membranes, limits the drug uptake and accumulation in both drug-sensitive and drug-resistant cells. As a result, liposomes with no encapsulated therapeutic agents could enhance the cytotoxicity of vinblastine (VLB) in CEM/VLB100 cells (vinblastine resistant) by around ten-fold and were even significantly more efficient than the efflux pump inhibitor, verapamil, alone. On the other hand, parent-sensitive CEM cells were unaffected by this liposome treatment. This led to the hypothesis that liposomal lipids inserted into the plasma membranes of resistant cells modified their characteristics and fluidity, allowing for a considerable restoration of drug accumulation with no effect on the rate of drug efflux from those cells.<sup>159</sup> The activation of apoptosis, the reduction of tumor volume, a decrease of ascites side effects, and longer life were also validated in mice treated intravenously with hybrid liposomes (HL-25) without any medications. These inhibitory effects on tumor cell proliferation should be linked to membrane fluidity.<sup>41</sup>

Some therapeutic medications require specific proteins to traverse plasma membranes or move across intracellular compartments, and drug resistance develops when their expression is reduced. By delivering therapeutic agents into cancer cells without relying on those particular proteins, nanoparticles can circumvent this resistance mechanism (Fig. 2). For example, because of various endocytic routes between cell lines,<sup>90,138</sup> the entrance mechanism or process of



the (cytarabine) Ara-CTP-dendrimer (nanoparticle) complex differs in different cells. Such behavior points to the dendrimer's role as a drug importation mechanism. Interestingly, this additional process does not exist in normal PBMCS, where the presence of the dendrimer hinders Ara-CTP activation.<sup>138</sup>

BCL2, an anti-apoptotic factor, has an important role in T-ALL cell survival. The combined treatment of DEX and GSI encapsulated in nanomaterial inhibited BCL2 expression more synergistically than the free combination model.<sup>136</sup>

**4.2.6. Therapeutic outcomes.** The access to *in vivo* tumor patterns that simulate the exact tumor environment of humans greatly determines the real outcomes of nanomedicines in a preclinical phase.<sup>86</sup> Animal models provide valuable data on biomedicine in pharmacological therapeutic studies.<sup>91</sup> Nanomedicine formulations encounter challenges such as loading therapeutic molecules into nanoparticles, maintaining nanoparticle formulation stability, and delivering encapsulated pharmaceuticals to the target region at the appropriate time *in vivo*. Furthermore, the shortage of acceptable animal models that replicate the actual clinical scenario in hematologic malignancies makes the exact prediction of clinical trial outcomes problematic.<sup>10,86</sup> The majority of current preclinical trials use xenogeneic models of immunodeficient animals to elude the destruction of human cells by the immune system, which does not precisely exhibit tumor microenvironments and does not present the immune system effects on tumor growth as well as nanoparticle targeting or efficacy.<sup>86,132</sup> The studies have not examined the influence of nano-drug formulation on angiogenesis as well, which is a measure used to predict late metastasis. Notwithstanding this, the studies assessed signs of overt leukemia (*viz.*, paraplegia or hepatosplenomegaly) for a long period.<sup>87</sup> The fluidic environment of the *in vivo* model frequently simulates complex hurdles, including fluid velocity, non-specific interactions with other cells or proteins, unintended nanoparticle dissemination, and quick clearance.<sup>108</sup> All in all, it was necessary to develop a proper animal model capable of more closely simulating leukemia and presenting a more thorough evaluation system.<sup>4,116</sup>

Most *in vivo* studies (14/18) included were prosperous in attacking and eliminating cancer cells *in vitro* (Table 3).<sup>17,108,109,111,120,121,129,132,133,136,144,146,148,160</sup> By analyzing therapeutic outcomes *in vivo*, researchers discovered that nano-drug encapsulations boosted anti-tumor activity compared to free chemotherapeutic drugs. Importantly, nanoparticles have been shown to pass the blood-brain barrier and circulate to sanctuary areas, such as the CNS, where higher medication exposure improves overall therapeutic effectiveness.<sup>93,150,160</sup> One immediate conclusion is that the high level of tumor uptake might clarify the suitable achievements of these formulations in lowering the tumor burden and increasing the survival rate.<sup>17,108,109,111,121,133,136,146,148,161,162</sup> This higher uptake by tumor, as previously referred to, can be attributed to the targeting moiety (sgc8, CD19, targeted tyrosine kinase, and transferrin receptor (TfR, also named CD71)) or stimuli-responsive behavior (pH and GSH-triggered) in some studies.<sup>108,120,121,129,133,134,136,144</sup>

In studies in which there are no bio-distribution details to realize tumor uptake or accumulation,<sup>87,120,144,163</sup> some properties of the formulations might indicate their treatment success. The pharmacokinetic index has clearly improved, with a longer circulation time and a small distribution mass restricted to plasma volume, decreased clearance, and better efficacy/toxicity profiles than free drugs.<sup>10</sup> To improve effectiveness, a threshold concentration in bone marrow must be reached and maintained for a long period.<sup>162</sup> The nanoparticles' distribution and accumulation level on different organs are strongly linked to their size or scale, the form of shape, and surface charge. Particles of 50–250 nm size mostly accumulated in the liver and spleen for several months, while only particles smaller than 10 nm accumulated and settled in other organs such as the kidneys, lungs, brain, and so on.<sup>15,160</sup> A long-time circulation would increase the chances of nanoparticles coming into contact with malign cells in the peripheral blood, a common target location in hematological malignancies. Nanomedicines tend to collect in the liver, spleen, and bone marrow as the mononuclear phagocytic system (MPS) organs annex to tumor sites.<sup>10</sup> These organs are also main and/or secondary target areas in most hematological malignancies, which can boost therapy effectiveness even more.<sup>10,17,109,133,160</sup> Furthermore, because nanoparticles accumulate less in active filtration organs such as the lungs and kidneys, encapsulated drugs may have a longer half-life than free drugs. Although the dosage employed in the mice did not result in a definite cure, it is notable that nanoparticle encapsulation considerably improved medication effectiveness at lower doses.<sup>17,133</sup> Although smaller particles have superior plasma profiles,<sup>133</sup> the drug encapsulation amount is limited by nanoparticles smaller than 50 nm.<sup>10</sup>

There is a long-term circulation of neutral nanocarriers in the blood. Nanocarriers with a negative charge are eliminated from Kupffer cells, whereas positively charged nanocarriers are removed *via* opsonization.<sup>89</sup> Scavenger receptors<sup>162</sup> facilitated the absorption of negatively charged nanoparticles (*e.g.*, liposomes)<sup>87,163</sup> by bone marrow macrophages. Polymeric micelles (PMs) composed of block copolymers with the hydrophilic shell ensure colloidal stableness and an elongated circulation *in vivo*.<sup>10,120</sup> The degree of PEGylation also influences bone marrow uptake. Slow liberation from long-flowing PEGylated liposomes, on the other hand, might reduce drug concentrations at the (main) desired site.<sup>10</sup>

Nanomedicines taken orally can be absorbed by microfold cells in Peyer's patches. This leads to improved systemic medication distribution and passive lymphatic targeting. Despite the higher therapeutic efficacy, Zou *et al.* found that nano-encapsulated 6-mercaptopurine (6-MP) had no sustained releasing impact *in vivo*. This phenomenon was described by the presence of esterase, which might breakdown the PLGA skeleton *via* the hydrolysis of ester bonds.<sup>111</sup> However, the methylated metabolite of 6-MP (6-MMP) may be harmful to the liver and BM. This study implied that hepatotoxicity and myelotoxicity were lower in the drug-nanoencapsulated group than in the free drug suspension group, owing to the avoidance of



Table 3 *In vivo* evaluation of therapeutic outcomes and toxicity of nanomaterials<sup>a</sup>

Nanomaterial	Drug, bioactive, photosensitizer, or gene	Therapeutic strategy	Animal model/cell line	Bio-distribution	Tumor growth inhibition (tumor ablation, recurrence)	Survival rate	Side effects (systematic toxicity, body weight, and histologic assessment)
Liposome <sup>163</sup>	Vincristine (VCR)	Liposomal vincristine 50–60 nm, 1 mg kg <sup>-1</sup> intraperitoneal	Xenograft NOD/SCID ND mice, B-ALL	20% delay in tumor progression	Increased lifespan	Enhanced	Antileukemic efficacy of the nano-drug
Liposome <sup>161</sup>	cytarabine : daunorubicin cocktail (300 : 4.5 mg kg <sup>-1</sup> )	CPX-351: Cyt: Daun 100 ± 20 nm, 10 : CCRF-CEM	SCID/Rag2M mice, constant tumor uptake (BM)	Considerable and	ND	Increased lifespan	Antileukemic efficacy compared to the free drug
Liposome <sup>162</sup>	cytarabine : daunorubicin cocktail (300 : 4.5 mg kg <sup>-1</sup> )	CPX-351: Cyt: Daun 10 : 4.4 mg kg <sup>-1</sup> i.v.	Xenograft Rag2-M mice, CCRF-CEM	Considerable and constant tumor uptake (BM)	Long-term remission in 33% of mice	Increases lifespan	Antileukemic efficacy compared to free-drug cocktail
Liposome-PEG <sup>87</sup>	WHIP131 (CAS 202475-60-3) JAK3 tyrosine kinase inhibitor/vincristine (VCR) 0.050 mg kg <sup>-1</sup> TBI treatment (200y γ-rays)	WHI-P131-NP 100 nm, 100 mg kg <sup>-1</sup> day <sup>-1</sup> × 2 days i.p.	Xenograft SCID mouse, resistant B-ALL RS4;11	ND	No signs of overt leukemia	Increased lifespan	Antileukemic efficacy compared to the free-drug cocktail
Liposomal Nanoformulation (LNF)-PEG <sup>146</sup>		C61-LNP 136.3 ± 1.2 nm, 80 mg kg <sup>-1</sup> i.v./C61-LNP + 2 Gy γ-rays	Xenograft NOD/SCID ND: favorable mouse, relapsed BPL, pharmacokinetic of i.v./C61-LNP + 2 Gy γ-xenograft NOD/SCID 25A <sup>145</sup>	ND	ND	Increased lifespan	Antileukemic efficacy compared to vincristine (VCR)
	TBI treatment (400y γ-rays)	C61-LNP 136.3 ± 1.2 nm, 80 mg kg <sup>-1</sup> i.v./C61-LNP + 4 Gy γ-rays	CD22ΔE12×BCR-ABL double-Tg mice, radiation-resistant BPL	Lower tumor growth/ remission C61-LNP + TBI mice: 100%, TBI: 50%, C61-LNP: (0)	Increased burden rate	Increased lifespan	Antileukemic efficacy compared to the free drug
Liposome-PEG <sup>109</sup>	Vincristine (VCR)	Sgc8-VCR-Lipo/VCR-Lipo 100 nm i.v.	Female BALB/c nude mice, CCRF-CEM	Liver tumor accumulation	Lower tumor growth/ burden rate	Increased lifespan	Antileukemic efficacy compared to the free drug

Table 3 (Contd.)

Nanomaterial	Drug, bioactive, photosensitizer, or gene	Therapeutic strategy	Animal model/cell line	Bio-distribution	Tumor growth inhibition (tumor ablation, recurrence)	Survival rate	Antileukemic efficacy of the nano-drug	Side effects (systematic toxicity, body weight, and histologic assessment)
PEG-PCL-ECT2 (amphiphilic block copolymers) <sup>17</sup>	Dexamethasone (Dex)	Dex-NP-PEG 110 nm, 5 mg kg <sup>-1</sup> i.v.	Xenograft NSG-B2m mice, human ALL	Spleen, liver accumulate, sustained plasma circulation, lower levels in the kidney and lung (clearance organs)	ND	Increase lifespan	Enhanced Antileukemic efficacy compared to the free drug	Well tolerated, safer
Amphiphilic block copolymers-PEG-PCL <sup>133</sup>	DOX (doxorubicin)	Anti-CD19-DOX-NPs 75 nm, 2.5 mg kg <sup>-1</sup> i.v.	Xenograft NSG-B2m mice, RS4; 11 B-ALL	BALB/c mice: liver, spleen accumulation (targeted NPs) with lower levels in clearance organs	ND	Increased lifespan	Enhanced Antileukemic efficacy compared to the free drug	Well tolerated, safer
PEG poly(lactic- <i>co</i> -glycolic acid) <sup>144</sup>	IRAK1/4 and ABT-737 cocktail	IRAK/ABT-PEG-PLGA polymer NP 100 nm, 10 mg kg <sup>-1</sup> IRAK inhibitor and 40 mg kg <sup>-1</sup> ABT-737 Sgc8-DOX-PRNCS-PEG i.v.	Xenograft female polymer NP 100 nm, NPG mice, Jurkat	ND	Lower tumor growth/ burden rate	Increased lifespan	Enhanced Antileukemic efficacy compared to the free drug	ND
Polyrotaxane-based nanoconstruct (PRNC), PEG <sup>108</sup>	DOX (doxorubicin)	Balb/c nude mice, CCRF-CEM	ND: rapid clearance of NPs	Lower tumor growth/ burden rate	ND	Enhanced Antileukemic efficacy compared to the free drug	Well tolerated, safer	Well tolerated, safer
Silver (AgNPs)-mesoporous silica nanospheres (MSNs)-PEG <sup>121</sup>	Paclitaxel (PTX)	Sgc8-PTX-MSNs-AgNPs-PEG 90 nm, i.v. 1 mg kg <sup>-1</sup>	BALB/c nude mice, CEM	Tumor accumulation	Lower tumor growth/ burden rate	ND	Enhanced Antileukemic efficacy compared to the free drug	Well tolerated, safer
Polymeric micelles (PCL-ss-Sgc8-BSA (polycaprolactone)) <sup>120</sup>	Ara-C 20 mg kg <sup>-1</sup>	Sgc8-PCL-ss-Ara-BSA 165.1 ± 5.2 nm, 20 mg kg <sup>-1</sup> i.v.	Tumor-bearing mice, ND	ND	Lower tumor growth/ burden rate	ND	Enhanced Antileukemic efficacy compared to the free drug	Well tolerated, safer
Polyl(beta-amino ester) (PBAE)	Plasmid DNA encoding the leukemia-specific 194-1BBz CAR-polymer-(microtubule) <sup>132</sup>	anti CD3-antiCD19- (PBAE)-(MTAS)-(NLS) 194-1BBz CAR (+HPB7 i.v. transposase).	Albino C57BL/6 mice, B-ALL (Eu-ALL01)	Liver accumulation (non-targeted NPs). Spleen, lymph nodes, bone marrow accumulation	Liver accumulation (targeted NPs)	Similar to the conventional CAR T-cell group	Similar to the conventional CAR T-cell group	Well tolerated, safer
		Infusion of 194-1BBz CAR-T cells transduced <i>ex vivo</i> with 194-1BBz-encoding lentivirus vectors						

Table 3 (Contd.)

Nanomaterial	Drug, bioactive, photosensitizer, or gene	Therapeutic strategy	Animal model/cell line	Bio-distribution	Tumor growth inhibition (tumor ablation, recurrence)	Survival rate	Side effects (systematic toxicity, body weight, and histologic assessment)
DMAP-EDCl-DMF + zinc( <sup>n</sup> ) phthalocyanine (ZnPc), (ZnPc), (photosensitizer: PS): C5 (ref. 129)	Dasatinib (small-molecule-tyrosine kinase inhibitor)	DMAP-EDCl-DMF + (ZnPc), (photosensitizer: PS): (PDT), tail vein	Nude mice, CCRF-CEM	Tumor accumulation. Rapid clearance of C4	Lower tumor growth/ ND	ND	Well tolerated, safer Antileukemic efficacy compared to the free drug under light exposure
Copolymer mPEG-PTMC <sup>160</sup>	Dexamethasone (Dex) 2.5–5 mg kg <sup>-1</sup>	mPEG-PTMC-Dex 41 nm, 5 mg kg <sup>-1</sup> i.v. ALL i.p.	NSG mice, primary T-lymphoma	Broad distribution. Accumulation in the major organs.	ND	ND	Enhanced Antileukemic efficacy compared to the free drug
PEG-PLA (polymeric micelles (PMS)) <sup>148</sup>	DOX (doxorubicin) 3 mg kg <sup>-1</sup> i.p.	DOX-PMs-NPMBP 3 mg kg <sup>-1</sup> i.p.	BALB/C-nude mice, Nalm6, resistance Nalm6 (B-ALL cell line)	Lower tumor growth/ ND	ND	ND	Enhanced Antileukemic efficacy compared to the free drug
PLGA <sup>111</sup>	6-Mercaptopurine (6-MP) 15.75 mg kg <sup>-1</sup> oral	PLGA-6-MP 138.01 ± 0.39 nm 15.75 mg kg <sup>-1</sup> oral	NCG mice, Nalm6, resistance Nalm6 (B-ALL cell line)	Lower tumor growth/ ND	ND	ND	Enhanced Antileukemic efficacy compared to the free drug
DSPE-PEG-DT7 (peptide-modified lecithin nanoparticles): TLnp <sup>13,6</sup>	Gamma-secretase inhibitors (GSIs) with dexamethasone (DEX): D&G-sol	DT7-DEX + GS1 co-loaded lecithin nanoparticles (TLnp/D&G) 32.36 ± 2.15 nm DEX 30 mg kg <sup>-1</sup> , GS1 30 mg kg <sup>-1</sup> i.v.	NSG, CEM	Tumor accumulation	Lower tumor growth/ Increased burden rate	Increased lifespan	Well tolerated, safer Enhanced Antileukemic efficacy compared to the free drug

<sup>a</sup> ND: not determined.

direct drug metabolism by liver microsomal enzymes after encapsulation.<sup>111</sup>

A combination of multiple drugs is frequently employed to attack the tumor cells by the restriction of several oncogenic pathways simultaneously. This often eventuates better anti-leukemic strategies with the drug's effective concentration in leukemia cells, resulting in their long-term death.<sup>10,136,144,161,162</sup> A 5 : 1 cytarabine : daunorubicin molar ratio revealed the reliable modulation of synergy and the lowest possibility of antagonism. In the combination model of the free cytarabine: daunorubicin cocktail, the administered drug ratios depicted an antagonistic couple *in vitro* after about two hours. The ratios could be kept for an extended period after administration *in vivo* by the encapsulated form of liposomes and retained the two combined drugs in the desired ratio pattern of their pharmacokinetics. CPX-351 illustrated a notable advancement in the therapeutic profile compared to the free-drug combination form. This strategy keeps the drug ratios away from antagonistic forms in the plasma and locations of growing tumors. When the amounts of drugs in individual liposomal cytarabine and individual liposomal daunorubicin were similar to those related to CPX-351 and tested in tumor-bearing mice, the efficacy obtained from CPX-351 was much better than in two separate liposomal drug agents.<sup>161,162</sup> Similarly, the co-delivery of DEX and GSI *via* nanocarriers reduced AKT (Ser473) phosphorylation and downregulated the anti-apoptotic protein BCL2, resulting in a considerable improvement in anti-leukemia efficacy.<sup>136</sup>

Metformin inhibits angiogenesis in certain cancers by acting synergistically with cisplatin. Specially formulated lipid-based cubosomal nanoformulations were utilized as drug carriers to promote chemical entrance in low dosages. Combining the medications in a carrier, on the other hand, had an antagonistic impact, indicating that metformin is not a viable alternative for sensitizing leukemia cells to cisplatin.<sup>164</sup>

Most therapeutic agents are also poorly soluble in water, wherein solubility limits absorption and nanoencapsulations offer them high solubility, which results in higher uptake and sustained release in tumor cells.<sup>111,144,145</sup> C61-LNP formulation (alone or in combination with irradiation) intensified the anti-leukemic power of low-dose TBI both *in vitro* and *in vivo*. It elevated the event-free survival time and the survival outcome in NOD/SCID mouse models of relapsed BPL more than in untreated control NOD/SCID mice or mice handled with two Gy single-dose TBI alone.<sup>145,146</sup> It is worth saying that the treatment protocol of C61-LNP formulation alone against CD22ΔE12 × BCR-ABL double-Tg mice (spontaneously expand radiation-resistant lethal BPL) was similar to the untreated ones.<sup>146</sup> The study did not notice any explanation for it. Additionally, the report was without biodistribution information, and thus it is arduous to describe the possible proofs why this formulation is not efficient. On the other hand, the *in vivo* NOD/SCID mouse model showed the anti-tumor efficacy of this agent.<sup>146</sup> In another previous study by the same authors, although there were no BM accumulation data, C61-LNP illustrated good pharmacokinetics and a harmless profile in mice.<sup>145</sup> Hence, it is believed that this cannot be relevant to the absence of tumor uptake. We can at least hypothesize some possible

factors like a larger tumor burden or the type of animal model in which a special BM microenvironment protects leukemic cells from nanoparticle encapsulation of targeted therapies. This protecting model might be an inducing factor of the malignant cell refractory.

**4.2.7. Toxicity.** Although nanoencapsulations minimize several key toxicities more than free chemotherapeutic drugs, additional toxicities can occur following the altered tissue distribution (*e.g.*, toxicities of the liver, spleen, bone marrow, and hand-foot syndrome).<sup>10,116</sup> If nanoparticles' active and functional surface is seen as a benefit for simple contact with medications, bioactives, genetic items, or other nanosystems, interaction with biological constructions will be feasible. Therefore, due to the toxicity concerns, it may be the most critical constraint.<sup>120</sup> The long circulation features of PEGylated liposomes, for example, may cause non-specific accumulation in the skin, resulting in noticeable unwanted effects. Furthermore, repeat injections of PEGylated nanoparticles can promote the development of anti-PEG IgM, changing pharmacokinetics and biodistribution. PEGylated NPs can also stimulate innate immunological reactions, enabling non-IgE-mediated complement activity and quicker blood elimination and pseudo-allergic responses.<sup>10</sup> The size and thickness of the particles, their surface charge, colloidal stability, and concentration have been shown to influence their biological toxicity significantly.<sup>12,164</sup> As a result, the primary criticism of several of the research studies considered in this analysis must be the shortage of information on the general toxicity or safety of nanomaterials (Table 3). The aggregation nature of less hydrophilic nanoparticles, especially under physiological status (*e.g.*, in serum), might have implications and be hazardous to various cells. The colloidal stability of nanoparticles can be enhanced by enclosing their surface with biocompatible materials that elevate water solubility and the body distribution of therapeutic agents. PEG covering is a common technique for achieving these goals, and it was utilized as a coverage and/or linker of target ligands in numerous investigations reviewed here (Tables 1 and 3). Other plans included enveloping nanoparticles with HAS<sup>74,94</sup> and BSA.<sup>120</sup> An HSA or BSA enveloping permits better flow in plasma and distribution throughout the body.

*In vitro* toxicity assessment needs a certain critical look. Several studies applied a cell line representative of healthful tissues to assess the cytotoxicity, and a cancer cell line was regarded for therapeutic assessments.<sup>50,94,103,104,107,108,115,118,119,121,128,133,134,141</sup> On the other hand, cancer cell lines might be more resistant or sensitive depending on their genotype. As a result, primary cell lines would be better for assessing cytotoxicity.<sup>12</sup>

*In vivo* toxicity evaluations were mostly based on histological tests of healthful tissues or monitoring of animal weight changes after treatment. No toxicity issues were noticed in any of the papers in which these evaluations were made (Table 3). In comparison to control animals, no significant changes were found in any of the cases, and all parameters were within the reference range. Some tests confirmed the compound's *in vivo* biosafety as well as the H&E staining findings of normal organ sections, which showed no clear symptoms of organ damage or



inflammation.<sup>111,129,136,148</sup> Although some studies have shown that nanoparticles can accumulate in the liver and kidneys,<sup>17,109,132,133,145,160</sup> the studies did not analyze important liver biochemical profiles such as serum measurements of alkaline phosphatase (ALP), alanine aminotransferase (ALT), aspartate transaminase (AST), or serum evaluation of blood urea nitrogen (BUN) and creatinine (CR) for the kidney to evaluate toxicity further. It is also critical to perform a hematological examination. Once more, just five of the 18 *in vivo* studies considered in this review had a hematological assessment.<sup>120,132,136,150,162</sup> One of them was *in vitro*,<sup>120</sup> in which the parameters were within the reference values. Lim *et al.*<sup>162</sup> assessed circulating platelets and bone marrow hematopoiesis and discovered toxicity related to the administration dose and schedule time. Elevated cytokines, such as tumor necrosis factor- $\alpha$  (TNF- $\alpha$ ), indicate toxicity as part of the inflammatory response after intravenous delivery.<sup>12</sup> By contrast, preclinical papers have primarily planned xenogeneic models of immunodeficient mice that do not precisely signify interactions between nanomedicines utilized with the immune system. This consideration was only seen in one among the 63 studies included in this review, and treatments based on nanoparticles aroused only modest expression levels of inflammatory cytokines (e.g., interferon-gamma, interleukin-12, and interleukin-6). Cell counts and blood chemistry parameters also illustrated no abnormalities, indicating that general toxicities did not occur.<sup>132</sup>

#### 4.3. Nanomaterials as diagnostics in ALL

**4.3.1. Cancer diagnostics on the nanoscale.** Imaging and molecular technologies, the most extensively used cancer detection tools, can only identify cancer after hundreds of cancer cells have grown and even metastasized. As a result, developing methods for detecting cancer at an early stage, before it spreads, is a significant issue. Nanotechnology-based diagnostic approaches are being developed as potential tools for cancer diagnosis and detection that are real-time, easy, and cost-effective. To identify cancer, nanoparticles are being utilized to gather cancer biomarkers.<sup>165</sup> For cancer diagnosis, nanoparticles provide a huge advantage in terms of the surface area to volume ratio.<sup>89,165</sup> Because of this feature, antibodies, aptamers, and other compounds that recognize specific cancer biomarkers can be extensively coated on nanoparticle surfaces. When several binding ligands are introduced into cancer cells, the specificity and sensitivity of an experiment may be increased, as can the ability to analyze many targets at once.<sup>165</sup> Nanoparticles utilized in cancer research, such as semiconductor nanocrystals, quantum dots, and iron oxide nanocrystals, exhibit optical, magnetic, and structural features that are not found in molecules or bulk materials. Besides, nanoparticles may easily adhere to the functional groups of various optical, radioisotopic, or magnetic diagnostic and therapeutic agents, making cancer detection more compelling and efficient.<sup>89</sup>

Table 4 Summary of studies using electrochemical biosensors

Cancer	Biosensor	Method	Sensitivity, quality and quantity	Advantage
ALL <sup>166</sup>	Electro-synthesized poly(catechol), graphene sheets, biosynthesized gold nanoparticles	Using DPV, EIS, CV, and chronoamperometry	Detection limits of 1.0 pM for the DNA strand	Continuous monitoring, molecular diagnosis of the BCR/ABL oncogene, and simple, rapid, and quantitative detection of many kinds of cancers
CML and ALL <sup>167</sup>	Polyaniline-gold composite	Molecular assay	A detection limit as low as $69.4 \times 10^{-18}$ M (41 DNA copies per $\mu$ L)	High specificity and selectivity
T-ALL <sup>119</sup>	Poly-HRP complex and CDNA-modified MNPs (CDN-MNPs) for miRNA detection	Conventional methods for detecting miRNA	Down to 100 fM in human serum	Process completion in a short time (about one hour)
Clinical cancer screening and early diagnosis <sup>170</sup>	Gold nanoparticles (AuNPs)	Scanning electrochemical microscopy (SECM)	The detection limit of $4.38 \times 10^{-12}$ M	Useful in the development for the detection of other antigens
Breast cancer, MCF-7 cell line (cell detection) <sup>169</sup>	Surface-enhanced Raman spectroscopic tagging material (SERS dots)	Raman signal	Specific for the targets	Molecular diagnosis of the BCR/ABL oncogene. Simple, rapid, and quantitative detection of many kinds of cancers
HeLa cells (human epithelial cervical cancer) and CERF- CEM cells (T cell) <sup>196</sup>	The FITC-FA-AuNPs (FFANPs)	Diphenyl alaninamide nanoparticles (FFANPs)	Sensitive detection of 10 000 HeLa cells by FCM assay of FFANPs	Simple and cost-effective
Human T-lymphoblast cell line MOLT-4 derived from patients with acute lymphoblastic leukemia <sup>197</sup>	Monoclonal antibody-targeted ZnO NRs	Flow cytometry	3 to 128 cells per $1.0 \text{ mm}^2$	Suitability for the detection of other relevant analytes



Table 5 Summary of studies using aptamers as biosensors

Cancer	Biosensor	Method	Sensitivity, quality and quantity	Advantage
Molt-4 cells <sup>198</sup>	Dual-aptamer (Sgc8c and ATP aptamers)-functionalized graphene oxide (DAFGO) complex	Flow cytometry analysis, fluorescence imaging	High targeting	Sensitive and selective detection of Molt-4 cells
ALL cells <sup>199</sup>	Specific DNA aptamer sgc8c	Topographic and recognition imaging (TREC)	High density and homogeneous lateral distribution in ALL-cells	Sensitive and selective detection of Molt-4 cells
CCL-119 cells <sup>180</sup>	Biotinylated aptamers in conjunction with metal-labeled neutravidin	Mass cytometry, CyTOF experiments	Differentiating positive, CCL-119, and negative, Ramos cell lines	Successfully utilized for mass cytometry experiments on par with commercially available antibodies
Ramos cells <sup>179</sup>	Aptamer-nanoparticle strip biosensor (ANSB)	SELEX (systematic evolution of ligands by exponential enrichment)	Detecting a minimum of 4000 Ramos cells without instrumentation and 800 Ramos cells with a portable strip reader	A simple, rapid, and low-cost tool for both the qualitative and quantitative detection of cancer
T-ALL cells <sup>185</sup>	Aptamer-conjugated magnetic beads (apt-MBs)	Magnet-QCM system	The detection limit of $8 \times 10^3$ cells mL <sup>-1</sup> for human acute leukemia cells	Required no further labeling of cells, the potential for specific detection of various kinds of cancer cells
Ramos cells <sup>184</sup>	Self-assembled aptamer-micelle nanostructure (TDO5-micelle)	Fluorescence shift	About 0.005 nM or 5 nM, based on DNA-lipid concentration	Rapid recognition ability with enhanced sensitivity and low critical micelle concentration
CCRF-CEM cells <sup>183</sup>	Single-stranded DNA aptamer	Gold nanoparticle (Au NP) labeling with backscattered electron (BE) imaging of field emission scanning electron microscopy (FESEM)	Sensitive and reversible probes to label target biomolecules on cells.	The high detection sensitivity of the colloidal probe method
HL-60 and CEM as AML and ALL cells <sup>182</sup>	Hierarchical assembly of dual aptamer functionalized, multilayered graphene-Au nanoparticle	Electrodeposition	The detection limit as low as 350 cells per mL, and a wide linear range	Diagnostic tool for early detection and classification of human acute leukemia
CEM and Ramos cells <sup>200</sup>	QDs-bsb-apt	Quantifying the fluorescence signal of the QDs	CEM cells (71.6%) could be detected by employing the QDs-bsb-Sgc8 complex, while FITC-Sgc8 detected 57.5% of cells	The detection efficiency of QDs-bsb-Sgc8 was 1.2-fold higher than that of the traditional organic dye modified aptamer FITC
CCRF-CEM cells <sup>201</sup>	Silver decahedral nanoparticle (Ag10NP)-based FRET (fluorescence resonance energy transfer) sensor (Ag10NP-based FRET sensor (Ag10-Sgc8-F/Q).	FRET-based methods	Highly sensitive and specific for CCRF-CEM cell imaging	Simple, inexpensive, and convenient for target cell imaging.
CCRF-CEM cells <sup>21</sup>	Terbium(III)-aptamer (Tb <sup>3+</sup> -apt)	Fluorescence spectrophotometer	The detection limit of 5 cells per ml of the binding buffer	Rapid, sensitive, and economical diagnosis of various types of leukemia at the early stage
CCRF-CEM cells <sup>202</sup>	ZnO nanodisks(NDs)@g-C <sub>3</sub> N <sub>4</sub> quantum dot conjugation to the Sgc8c aptamer	Photoelectrochemical (PEC)	The detection limit down to 20 cell per mL	Wide detection range, low detection limit, excellent selectivity, and reproducibility
ALL <sup>186</sup>	Aptamer-based electrochemical nano-biosensor (graphitic carbon nitride (Au/g-C <sub>3</sub> N <sub>4</sub> /aptamer nanocomposite)	Gene detection (miRNA-128)	The limit of detection of 0.0034 fM concentration of miRNA-128 detection	Needed a short time (about 45 minutes) to detect miRNA-128 as a symptom of the disease
CEM cells and Ramos cells <sup>203</sup>	Aptamer-functionalized copolymer/TPdye fluorescent organic dots	Two-photon imaging	Tissue imaging up to 210 mm	A powerful tool for cancer cell-targeted imaging



### 4.3.2. Nanoparticle-based biosensors for ALL detection

**4.3.2.1. Biosensor classification based on the type of transducer.** Hematological cancers, such as acute leukemia, may now be better diagnosed and treated because of the development of biosensors. Biosensors can be classified into optical, mass-based, calorimetric, and electrochemical types based on the type of transducer (Table 4). Enzymes, antibodies, cells, nucleic acids, and aptamers may be utilized as biosensor bio-components for analyte identification. Nanoparticle-based biosensors provide great sensitivity and specificity for developing any type of biosensor. Polyaniline nanofibers (PANI-NFs) are more attractive biosensors due to higher conductivity, lower cytotoxicity, and better biocompatibility. Stability in immobilized live cells and strong electrical characteristics are further advantages of gold nanoparticles (AuNPs). AuNPs/PANI-NF nanocomposites are excellent in the immobilization of cells. Biosensors based on a polyaniline–gold composite can detect biomarkers in the range of  $10^{-18}$  M.<sup>166–172</sup> Moreover, these biosensors are used in the specific and quantitative detection of many kinds of cancers by targeting molecular and cellular diagnosis levels. According to prior investigations, a biosensor including folic acid (FA) and AuNPs was able to identify  $10^4$  cancer cells at a level equivalent to flow cytometry (FCM).

DNA-based aptamers may be used as biosensors in the same way as antibodies but with greater selectivity and affinity for certain biomarkers (Table 5).<sup>173</sup> In clinical applications, to ensure the reliability of the positive result of a DNA test, an aptamer test will be used. Aptamer-modified nanomaterials such as aptamer modified Quantum Dots (QDs), AuNPs, dye-doped silica NPs, and magnetic nanoparticles (MNPs) are extremely useful diagnostic tools for specific targets with more efficient function than aptamer free modification with nanomaterials. Aptamers' optical, electrochemical, magnetic, and mechanical capabilities, as well as the ease with which they may be synthesized, modified, and tailored to work with different detection modalities, all contribute to their great efficiency in recognizing and delivering drugs to target cells.<sup>174</sup>

Biosensor-based nanoparticles have superior properties, including electron transfer facilitation, unique optical and plasmonic effects, biocompatibility, and an excellent affinity for biomolecules, facilitating the immobilization of antibodies, enzymes, nucleic acids, and proteins, compared with their bulk counterparts.<sup>175,176</sup>

**4.3.2.2. Biosensor classification based on the identification purposes.** Biosensors are divided into three categories based on their identification purposes. The first cellular target identifies cancer stem cells, whose sensitivity and specificity are expressed by identifying the number of cells per milliliter. For this purpose, many studies have been done. Using an aptamer-based electrochemical biosensor (sgc8c aptamer–gold nanoparticle-coated magnetic  $\text{Fe}_3\text{O}_4$  nanoparticles (Apt-GMNPs)), a highly sensitive, selective, and simple method for early-stage detection of leukemia cancer was introduced. So, specifically targeting the cells of interest by using modified nanoparticles improved sensitivity detection by limiting detection as low as ten cells per ml.<sup>177</sup> The second identified cancer cells based on peptide or protein targets and even related chemical metabolites, in which sensitivity and accuracy are expressed as a unit of concentration. In this regard, an apta-sensor with a self-assembled aptamer–micelle nanostructure (TDO5-micelle) can detect DNA-lipid concentrations as low as 0.005 nM.<sup>21,65,178–185</sup> The third one is nucleic acid targets such as biomarker microRNAs or other non-coding DNA/RNAs. Depending on the method used, the sensitivity and specificity may be expressed in terms of the copy number or something similar. Nanoparticles may be enhanced by employing carriers for targeting, such as integrating nano-designs with organ-specific response receptors.<sup>119</sup> An aptamer-based electrochemical nano-biosensor demonstrates efficacy in the early identification of ALL by gene detection (microRNA-128). In this work, Graphitic Carbon Nitride ( $\text{G-C}_3\text{N}_4$ ) has been used in the square wave voltammetry (SWV) technique. The LOD of this nano-complex was obtained to be about 0.0034 fM. So, electrochemical biosensors show suitable practical application prospects for analyzing miRNAs with high sensitivity.<sup>186,187</sup> Until

Table 6 Summary of studies using biosensors for mercaptopurine detection

Cancer	Biosensor	Method	Sensitivity, quality and quantity	Advantage
ALL <sup>168</sup>	6-Thiouric acid	Electrochemical surface-enhanced Raman spectroscopy (EC-SERS)	Excellent signal for 6-TUA down to $\mu\text{M}$ concentrations in synthetic urine	Detected rapidly at clinically relevant concentrations, without the need for sample pre-treatment (less than 1 minute)
ALL <sup>204</sup>	Chip-based capillary electrophoresis (CE) (CE-EC detection)	PMMA-based microfluidic chip	The detection limit of 100 nM	High detection speed, negligible sample consumption, low power requirement, easy integration
ALL <sup>171</sup>	Gold nanoparticles (AuNPs)	SPR	More sensitive for detecting different purines at a concentration of $10^{-7}$ M for 6-thioguanine and 6-mercaptopurine	High detection speed, negligible sample consumption, low power requirement, and easy integration



now, various types of biosensors such as electrochemical (EC) methods, chemiluminescence (CL) high-performance liquid chromatography (HPLC), UV-vis spectrophotometry, surface-enhanced Raman scattering spectroscopy and other methods were used for 6-mercaptopurine detection in order to monitor the concentrations of 6-mercaptopurine in human serum (Table 6). It is remarkable that fluorescent nanosensors were developed for this purpose with an acceptable detection limit (0.198 nM).<sup>188–190</sup>

Many hurdles, including reliability, repeatability, quantitative detection findings, and biosafety, must be overcome to expedite the translation of nanotechnology as a diagnostic tool into clinical applications. Nonspecific nanoparticle probe binding, aggregation, and unsuitable detection circumstances are only a few issues that might impact nanoparticle-based detection results. Signal fluctuations can also be due to the complex makeup of bodily fluids.<sup>165</sup>

## 5 Conclusion

This study examined nanomedicines' recent benefits and drawbacks, advances in drug delivery, and modern diagnostic approaches.<sup>24,191</sup> Originally, nanotechnology usage greatly relied on solubility and absorption improvement, bioavailability, extended blood circulation time, targeting strategy, and sensitive or controlled-release drug agents.<sup>91</sup> The aim is to enhance treatment efficacy and alleviate the general toxicity. The co-loading of several drug agents may help abolish the restrictions in which drugs are impossible to administer at the same time and reduce the refractory to the therapeutic drug. The real-time following of this system is feasible *via* processing the biological probing agents.<sup>4</sup> Nanoparticles can be effective in overcoming the MDR problem.<sup>10</sup> Progressions in nanotechnology development enable the loading of higher intracellular concentrations of drug agents and, consequently, improve their effectiveness. Finally, even by reducing drug consumption, this strategy helps achieve a constant and longer remission duration in patients.<sup>192</sup>

A variety of nanoparticle-based assays improved diagnostic selectivity and sensitivity or added whole new capabilities, such as easy analysis, that were not possible with older methods. These advancements will enhance cancer patient survival rates by allowing early identification, leading to improved cancer treatment options.<sup>86,165</sup> Even integrating diagnosis with treatment strategies is also coming to the real world.<sup>91</sup> Nanotechnology can provide the possibility of diagnostics accompanied by the treatment scanning of hematologic malignancies in real time.<sup>4,86</sup>

Both *in vitro* and animal studies have presented a valuable picture for realizing the illness behavior and nanomaterial interactions with alive tissues or efficacy on malignant cells.<sup>193</sup> Nonetheless, we are yet in the experimental phase and investigational stage in the field of nanomedicine or nanotechnology. We must evaluate some features and overcome numerous problems, such as biocompatibility, long-term toxicity, immunogenicity, targeting, pharmacokinetics, biodistribution and clearance pathways of the entire nanoparticles, and inadequate

drug release response before entering clinical applications.<sup>4</sup> Generally, the experimental conditions of nanoparticle efficacy assessment against leukemia vary considerably between different preclinical studies in addition to shortage evaluation of *in vivo* stability, toxicity, safety, and biodistribution, which results in their lower and variable clinical impact.<sup>86</sup> There may also be some issues with the drug-responsive liberation process, like an irreversible stimulus-response and low targeting. The scarcity of exact animal models to mimic leukemia more closely affects the accurate evaluation of the leukemia mechanism [4], making it difficult to anticipate their successful results for clinical trials.<sup>10</sup>

## Author contributions

Re. K. conceptualized the study, searched the databases, screened the literature, reviewed the studies, extracted the data, assessed the included studies' quality, and prepared the original draft of the treatment section. Z. M. extracted the data, assessed the included studies' quality, and prepared the original draft of the diagnosis section. Ra. K. conceptualized the study, searched the databases, screened the literature, extracted the data, and designed the graphical abstract. A. S. conceptualized the study and edited the manuscript. N. R. conceptualized the study, appraised the manuscript, and supervised the project.

## Conflicts of interest

The authors have no conflicts of interest to disclose.

## Acknowledgements

The authors would like to thank Dr Malakeh Malekzadeh for her assistance with research in the diagnosis section.

## References

- 1 R. Yazdian-Robati, A. Arab, M. Ramezani, K. Abnous and S. M. Taghdisi, *Int. J. Pharm.*, 2017, **529**, 44–54.
- 2 M. Houshmand, F. Garello, P. Circosta, R. Stefania, S. Aime, G. Saglio and C. Giachino, *Nanomaterials*, 2020, **10**.
- 3 V. Cordo, J. C. G. van der Zwet, K. Canté-Barrett, R. Pieters and J. P. P. Meijerink, *Blood Cancer Discov.*, 2021, **2**, 19–31.
- 4 J. Shen, Z. Lu, J. Wang, T. Zhang, J. Yang, Y. Li, G. Liu and X. Zhang, *ACS Biomater. Sci. Eng.*, 2020, **6**, 6478–6489.
- 5 Z. Hong, Z. Wei, T. Xie, L. Fu, J. Sun, F. Zhou, M. Jamal, Q. Zhang and L. Shao, *J. Hematol. Oncol.*, 2021, **14**, 48.
- 6 R. Stephenson and A. Singh, *Adv. Drug Delivery Rev.*, 2017, **114**, 285–300.
- 7 L. V. Cappelli, D. Fiore, J. M. Phillip, L. Yoffe, F. Di Giacomo, W. Chiu, Y. Hu, C. Kayembe, M. Ginsberg, L. Consolino, J. G. Barcia Durán, N. Zamponi, A. M. Melnick, F. Boccalatte, W. Tam, O. Elemento, S. Chiaretti, A. R. Guarini, R. Foà, L. Cerchietti, S. Rafii and G. G. Inghirami, *Blood*, 2022, DOI: [10.1128/blood.2022015414](https://doi.org/10.1128/blood.2022015414).



8 C. Thakur, P. Nayak, V. Mishra, M. Sharma and G. K. Saraogi, in *Nano Drug Delivery Strategies for the Treatment of Cancers*, ed. A. K. Yadav, U. Gupta and R. Sharma, Academic Press, 2021, pp. 225–243, DOI: [10.1016/B978-0-12-819793-6.00010-2](https://doi.org/10.1016/B978-0-12-819793-6.00010-2).

9 R. Basha, N. Sabnis, K. Heym, W. P. Bowman and A. G. Lacko, *Front. Oncol.*, 2014, **4**, 101.

10 A. K. Deshantri, A. V. Moreira, V. Ecker, S. N. Mandhane, R. M. Schiffelers, M. Buchner and M. Fens, *J. Controlled Release*, 2018, **287**, 194–215.

11 G. Visani, F. Loscocco and A. Isidori, *Nanomedicine*, 2014, **9**, 2415–2428.

12 T. Viseu, C. M. Lopes, E. Fernandes, M. E. C. D. R. Oliveira and M. Lúcio, *Pharmaceutics*, 2018, **10**(4), 282.

13 A. Andleeb, A. Andleeb, S. Asghar, G. Zaman, M. Tariq, A. Mehmood, M. Nadeem, C. Hano, J. M. Lorenzo and B. H. Abbasi, *Cancers*, 2021, **13**, 2818.

14 C. Wang, W. Zhang, Y. He, Z. Gao, L. Liu, S. Yu, Y. Hu, S. Wang, C. Zhao, H. Li, J. Shi, W. Zhou, F. Li, H. Yue, Y. Li, W. Wei, G. Ma and D. Ma, *Nat. Nanotechnol.*, 2021, **16**, 1413–1423.

15 A. S. Tatar, T. Nagy-Simon, C. Tomuleasa, S. Boca and S. Astilean, *J. Contr. Release*, 2016, **238**, 123–138.

16 F. Asghari, R. Khademi, F. Esmaeili Ranjbar, Z. Veisi Malekshahi and R. Faridi Majidi, *Int. J. Stem Cells*, 2019, **12**, 227–239.

17 V. Krishnan, X. Xu, S. P. Barwe, X. Yang, K. Czynnemek, S. A. Waldman, R. W. Mason, X. Jia and A. K. Rajasekaran, *Mol. Pharm.*, 2013, **10**, 2199–2210.

18 C. Cao, N. Yang, H. Dai, H. Huang, X. Song, Q. Zhang and X. Dong, *Nanoscale Adv.*, 2021, **3**, 106–122.

19 T. Limongi, F. Susa and V. Cauda, *Hematol. Med. Oncol.*, 2019, **4**, 1000183.

20 Y. Zhong, K. Beimnet, Z. Alli, A. Arnoldo, P. E. Kowalski, G. R. Somers, C. Hawkins and M. Abdelhaleem, *J. Mol. Diagn.*, 2020, **22**, 72–80.

21 S. Wu, N. Yang, L. Zhong, Y. Luo, H. Wang, W. Gong, S. Zhou, Y. Li, J. He and H. Cao, *Analyst*, 2019, **144**, 3843–3852.

22 B. B. Lundberg, *Int. J. Pharm.*, 2011, **408**, 208–212.

23 A. Wicki, D. Witzigmann, V. Balasubramanian and J. Huwyler, *J. Contr. Release*, 2015, **200**, 138–157.

24 G. Soni and K. S. Yadav, *Mater. Sci. Eng. C*, 2015, **47**, 156–164.

25 Y. Ye, J. Wang, Q. Hu, G. M. Hochu, H. Xin, C. Wang and Z. Gu, *ACS Nano*, 2016, **10**, 8956–8963.

26 R. S. Riley, C. H. June, R. Langer and M. J. Mitchell, *Nat. Rev. Drug Discovery*, 2019, **18**, 175–196.

27 J. J. Lee, L. Saiful Yazan and C. A. Che Abdullah, *Int. J. Nanomed.*, 2017, **12**, 2373–2384.

28 R. Vinhas, M. Cordeiro, F. F. Carlos, S. Mendo, A. R. Fernandes, S. Figueiredo and P. V. Baptista, *Nanobiosensors Dis. Diagnosis*, 2015, **4**, 11.

29 P. Pedrosa, R. Vinhas, A. Fernandes and P. V. Baptista, *Nanomaterials*, 2015, **5**, 1853–1879.

30 W. Mekseriwattana, P. Guardia, B. T. Herrero, J. M. de la Fuente, C. Kuhakarn, A. Roig and K. P. Katewongsa, *Nanoscale Adv.*, 2022, **4**, 1988–1998.

31 B. Ramdass, A. Chowdhary and P. S. Koka, *J. Stem Cell.*, 2013, **8**, 151–187.

32 D. Moher, A. Liberati, J. Tetzlaff and D. G. Altman, *PLoS Med.*, 2009, **6**, e1000097.

33 K. F. Schulz, D. G. Altman and D. Moher, *BMC Med.*, 2010, **8**, 18.

34 T. Ouchi, H. Kobayashi and T. Banba, *Br. Polym. J.*, 1990, **23**, 221–228.

35 Y. Ohya, K. Nonomura and T. Ouchi, *J. Bioact. Compat. Polym.*, 1995, **10**, 223–234.

36 M. S. Webb, A. H. Sarris, F. Cabanillas, L. D. Mayer, M. B. Bally, C. Burge and P. R. Cullis, *J. Liposome Res.*, 2000, **10**, 501–512.

37 A. K. Sharma, L. Zhang, S. Li, D. L. Kelly, V. Y. Alakhov, E. V. Batrakova and A. V. Kabanov, *J. Controlled Release*, 2008, **131**, 220–227.

38 N. Eslahi, A. Shakeri-Zadeh, K. Ashtari, V. Pirhajati-Mahabadi, T. T. Moghadam, R. Shabani, K. Kamrava, Z. Madjd, C. Maki, H. R. Asgari and M. Koruji, *Cell J.*, 2019, **21**, 14–26.

39 J. Koechling, Y. Rott, S. Anidt, J. Green, D. Anderson, R. Langer, R. Stripecke, B. Wittig and M. Schmidt, *Blood*, 2007, **110**, 366B.

40 Y. Tong, C. Li, F. Liang, J. Chen, H. Zhang, G. Liu, H. Sun and J. H. T. Luong, *Nucl. Instrum. Methods Phys. Res., Sect. B*, 2008, **266**, 5041–5046.

41 H. Ichihara, J. Ueno, M. Umebayashi, Y. Matsumoto and R. Ueoka, *Int. J. Pharm.*, 2011, **406**, 173–178.

42 F. A. Fakhr, A. Khanafari, M. Baserisalehi, R. Yaghoobi and S. Shahghasempour, *Afr. J. Microbiol. Res.*, 2012, **6**, 6235–6242.

43 D. Pramanik, N. R. Campbell, S. Das, S. Gupta, V. Chenna, S. Bisht, P. Sysa-Shah, D. Bedja, C. Karikari, C. Steenbergen, K. L. Gabrielson, A. Maitra and A. Maitra, *Oncotarget*, 2012, **3**, 640–650.

44 N. Satake, G. Barisone, E. Diaz, N. Nitin, J. Nolta and K. Lam, *Proceedings of SPIE - the International Society for Optical Engineering*, Baltimore, MD, 2012.

45 M. A. Orlova, E. Y. Osipova, S. A. Rumiantsev and D. A. Zaitsev, *Russ. Chem. Bull.*, 2013, **62**, 1120–1124.

46 R. Raghunathan, S. Mahesula, K. Kancharla, P. Janardhanan, Y. L. Jadhav, R. Nadeau, G. P. Villa, R. L. Cook, C. M. Witt, J. A. Gelfond, T. G. Forsthuber and W. E. Haskins, *Particle & particle systems characterization : measurement and description of particle properties and behavior in powders and other disperse systems*, 2013, vol. 30, pp. 355–364.

47 M. A. Orlova, A. A. Poloznikov and A. P. Orlov, *Moscow Univ. Chem. Bull.*, 2014, **69**, 142–147.

48 M. G. Kim, J. Y. Park, W. Miao, J. Lee and Y. K. Oh, *Biomaterials*, 2015, **48**, 129–136.

49 T. Pivetta, V. Lallai, E. Valletta, F. Trudu, F. Isaia, D. Perra, E. Pinna and A. Pani, *J. Inorg. Biochem.*, 2015, **151**, 107–114.



50 F. M. Uckun, H. Ma, J. Cheng, D. E. Myers and S. Qazi, *Br. J. Haematol.*, 2015, **169**, 401–414.

51 F. M. Uckun, L. G. Mitchell, S. Qazi, Y. Liu, N. Zheng, D. E. Myers, Z. Song, H. Ma and J. Cheng, *EBioMedicine*, 2015, **2**, 649–659.

52 Y. Matsumoto, K. Kuwabara, H. Ichihara and M. Kuwano, *Bioorg. Med. Chem. Lett.*, 2016, **26**, 301–305.

53 Z. Hasanzade and H. Raissi, *Appl. Surf. Sci.*, 2017, **422**, 1030–1041.

54 J. H. Kang, K. R. Kim, H. Lee, D. R. Ahn and Y. T. Ko, *Colloids Surf. B Biointerfaces*, 2017, **157**, 424–431.

55 S. Chen, J. Zaifman, J. A. Kulkarni, I. V. Zhigaltsev, Y. K. Tam, M. A. Ciufolini, Y. Y. C. Tam and P. R. Cullis, *J. Contr. Release*, 2018, **286**, 46–54.

56 S. Kallus, B. Englinger, J. Senkiv, A. Laemmerer, P. Heffeter, W. Berger, C. R. Kowol and B. K. Keppler, *Nanomed. Nanotechnol. Biol. Med.*, 2018, **14**, 2632–2643.

57 R. R. Nair, D. Piktel, W. J. Geldenhuys and L. F. Gibson, *Leuk. Res.*, 2018, **72**, 59–66.

58 A. C. Uscanga-Palomeque, K. M. Calvillo-Rodriguez, L. Gomez-Morales, E. Larde, T. Denefle, D. Caballero-Hernandez, H. Merle-Beral, S. A. Susin, P. Karoyan, A. C. Martinez-Torres and C. Rodriguez-Padilla, *Cancer Sci.*, 2019, **110**, 256–268.

59 S. Zong, L. Wang, Z. Yang, H. Wang and Z. Wang, *ACS Appl. Mater. Interfaces*, 2019, **11**, 5896–5902.

60 H. Al Faruque, E. S. Choi, H. R. Lee, J. H. Kim, S. Park and E. Kim, *Nanoscale*, 2020, **12**, 2773–2786.

61 M. Mohseni, C. Kucharski, K. C. R. Bahadur, M. Nasrullah, X. Y. Jiang, H. Uludag and J. Brandwein, *PLoS One*, 2021, **16**.

62 Y. A. Grechkin, S. L. Grechkina, E. A. Zaripov, S. V. Fedorenko, A. R. Mustafina and M. V. Berezovski, *Biomedicines*, 2020, **8**, 14.

63 N. F. Ramandi, I. S. Mashhadi, A. Sharif, N. Saeedi, M. A. Ashabi, M. Faranoush, A. GhassemPour and H. Y. Aboul-Enein, *J. Chromatogr. B*, 2022, **1190**, 123091.

64 X. Hu, Y. Wang, X. Zuping, P. Song, A. J. Wang, Z. Qian, P. X. Yuan, T. Zhao and J. J. Feng, *Anal. Chem.*, 2022, **94**, 3708–3717.

65 D. Woods, K. Winchester, A. Towerman, K. Gettinger, C. Carey, K. Timmermann, R. Langley and E. Browne, *J. Pediatr. Oncol. Nurs.*, 2017, **34**, 387–396.

66 M. Ramachandran, A. Dimberg and M. Essand, The cancer-immunity cycle as rational design for synthetic cancer drugs: Novel DC vaccines and CAR T-cells, in *Seminars in Cancer Biology*, Elsevier, 2017, pp. 23–35.

67 S. Sarangapani, R. E. Mohan, A. Patil, M. J. Lang and A. Asundi, presented in 5th International Conference on Optical and Photonics Engineering, *International Society for Optics and Photonics*, 2017, p. 1044936.

68 X. Li, B. Zhou, Z. Zhao, Z. Hu, S. Zhou, N. Yang, Y. Huang, Z. Zhang, J. Su and D. Lan, *J. Biomed. Nanotechnol.*, 2016, **12**, 2151–2160.

69 P. S. Kedar, V. Gupta, P. Warang, A. Chidharwar and M. Madkaikar, *Hematology*, 2018, **23**, 567–573.

70 E. A. Motea, I. Lee and A. J. Berdis, *ACS Chem. Biol.*, 2012, **7**, 988–998.

71 D. Shangguan, Z. Cao, L. Meng, P. Mallikaratchy, K. Sefah, H. Wang, Y. Li and W. Tan, *J. Proteome Res.*, 2008, **7**, 2133–2139.

72 J. Skulan, T. Bullen, A. D. Anbar, J. E. Puzas, L. Shackelford, A. LeBlanc and S. M. Smith, *Clin. Chem.*, 2007, **53**, 1155–1158.

73 H. Wang, H. Zeng, G. Shen and R. Yu, *Anal. Chem.*, 2006, **78**, 2571–2578.

74 B. Patra, A. K. Mishra and R. S. Verma, *J. Sci. Adv. Mater. Dev.*, 2022, **7**.

75 J. D. Cohen and H. I. Robins, *Cancer Res.*, 1987, **47**, 4335–4337.

76 P. Jungmayr and T. Müller-Bohn, *Dtsch. Apoth. Ztg.*, 2007, **147**, 66–73.

77 Y. Godfrin, *Innov. Pharm. Technol.*, 2009, 60–62.

78 K. I. Batarseh, *Curr. Med. Chem.*, 2013, **20**, 2363–2373.

79 A. A. Philchenkov, E. D. Shishko, M. P. Zavelevich, L. M. Kuiava, K. Miura, D. Y. Blokhin, I. O. Shton and N. F. Gamaleia, *Exp. Oncol.*, 2014, **36**, 241–245.

80 H. Pan, S. Li, M. Li, Q. Tao, J. Jia, W. Li, L. Wang, Z. Guo, K. Ma, Y. Liu and C. Cui, *Pharmazie*, 2020, **75**, 318–323.

81 J. Varshosaz, S. Fardshouraki, M. Mirian, L. Safaeian, S. Jandaghian and S. Taymouri, *Anti Cancer Agents Med. Chem.*, 2020, **20**, 1966–1980.

82 K. Sumi, K. Tago, Y. Nakazawa, K. Takahashi, T. Ohe, T. Mashino and M. Funakoshi-Tago, *Eur. J. Pharmacol.*, 2022, 916.

83 Y. F. Zhang, J. N. An, Y. Shao, N. Yu, S. J. Yue, H. L. Sun, J. B. Zhang, W. X. Gu, Y. F. Xia, J. P. Zhang, Y. Xu and Z. Y. Zhong, *Biomacromolecules*, 2022, **23**, 377–387.

84 P. Nandy, A. P. Pericloud and V. I. Avramis, *Anticancer Res.*, 1998, **18**, 727–737.

85 L. Mayer, H. Carol, C. L. Morton, T. Harasym, M. A. Smith and R. B. Lock, *Mol. Cancer Therapeut.*, 2009, **8**.

86 R. Vinhas, R. Mendes, A. R. Fernandes and P. V. Baptista, *Front. Bioeng. Biotechnol.*, 2017, **5**, 79.

87 F. M. Uckun, I. Dibirdik, S. Qazi and S. Yiv, *Arzneim.-Forsch.*, 2010, **60**, 210–217.

88 W. M. Becicka, P. A. Bielecki, M. E. Lorkowski, T. J. Moon, Y. Zhang, P. U. Atukorale, G. Covarrubias and E. Karathanasis, *Nanoscale Adv.*, 2021, **3**, 4961–4972.

89 V. K. Chaturvedi, A. Singh, V. K. Singh and M. P. Singh, *Curr. Drug Metab.*, 2019, **20**, 416–429.

90 M. Szwed, A. Matusiak, A. Laroche-Clary, J. Robert, I. Marszalek and Z. Jozwiak, *Toxicol. Vitro*, 2014, **28**, 187–197.

91 J. K. Patra, G. Das, L. F. Fraceto, E. V. R. Campos, M. d. P. Rodriguez-Torres, L. S. Acosta-Torres, L. A. Diaz-Torres, R. Grillo, M. K. Swamy, S. Sharma, S. Habtemariam and H.-S. Shin, *J. Nanobiotechnol.*, 2018, **16**, 71.

92 B. V. Lima, M. J. Oliveira, M. A. Barbosa, R. M. Gonçalves and F. Castro, *Biomater. Sci.*, 2021, **9**, 3209–3227.

93 H. Nekounam, R. Dinarvand, R. Khademi, R. Karimi, H. Arzani, N. Mahmoodi, E. Hasanzadeh, M. Kamali, M. Khosravani, *bioRxiv*, 2021, bioRxiv:2021.2005.2015.444280, DOI: [10.1101/2021.05.15.444280](https://doi.org/10.1101/2021.05.15.444280).



94 S. M. Taghdisi, N. M. Danesh, M. Ramezani and K. Abnous, *RSC Adv.*, 2016, **6**, 46366–46371.

95 C. Chittasupho, C. Aonsri and W. Imaram, *Bioorg. Chem.*, 2021, **107**.

96 H. Zhao, H. Wang, H. Li, T. Zhang, J. Zhang, W. Guo, K. Fu and G. Du, *Nanoscale Adv.*, 2022, **4**, 1815–1826.

97 A. G. Leonel, A. A. P. Mansur, S. M. Carvalho, L. E. F. Outon, J. D. Ardisson, K. Krambrock and H. S. Mansur, *Nanoscale Adv.*, 2021, **3**, 1029–1046.

98 L. Zhou, Y. Zhang and Y. Ma, *Nanoscale Adv.*, 2022, **4**, 4059–4065.

99 A. F. Chamorro Rengifo, N. Stefanés, J. Toigo, C. Mendes, M. C. Santos-Silva, R. J. Nunes, A. L. Parize and E. Minatti, *Mater. Sci. Eng. C*, 2019, **105**, 110051.

100 P. E. Feuser, P. C. Gaspar, A. V. Jacques, A. C. Tedesco, M. C. D. Santos Silva, E. Ricci-Junior, C. Sayer and P. H. H. de Araujo, *Mater. Sci. Eng. C*, 2016, **60**, 458–466.

101 P. E. Feuser, P. C. Matos dos Santos, A. P. Cordeiro, N. M. Stefanés, L. O. Walter, M. F. Maioral, M. C. Santos-Silva, P. H. Hermes de Araújo and C. Sayer, *J. Drug Deliv. Sci. Technol.*, 2022, **67**.

102 H. S. Rahman, A. Rasedee, C. W. How, A. B. Abdul, N. A. Zeenathul, H. H. Othman, M. I. Saeed and S. K. Yeap, *Int. J. Nanomed.*, 2013, **8**, 2769–2781.

103 N. M. Danesh, P. Lavaee, M. Ramezani, K. Abnous and S. M. Taghdisi, *Int. J. Pharm.*, 2015, **489**, 311–317.

104 S. M. Taghdisi, N. M. Danesh, P. Lavaee, A. S. Emrani, K. Y. Hassanabad, M. Ramezani and K. Abnous, *Mater. Sci. Eng. C*, 2016, **61**, 753–761.

105 K. Saravananakumar, E. Jeevithan, R. Chelliah, K. Kathiresan, W. Wen-Hui, D. H. Oh and M. H. Wang, *Int. J. Biol. Macromol.*, 2018, **119**, 1144–1153.

106 Y. F. Huang, D. Shangguan, H. Liu, J. A. Phillips, X. Zhang, Y. Chen and W. Tan, *Chembiochem*, 2009, **10**, 862–868.

107 S. M. Taghdisi, P. Lavaee, M. Ramezani and K. Abnous, *Eur. J. Pharm. Biopharm.*, 2011, **77**, 200–206.

108 D. Jang, Y. M. Lee, J. Lee, J. Doh and W. J. Kim, *Sci. Rep.*, 2017, **7**, 40739.

109 S. Duan, Y. Yu, C. Lai, D. Wang, Y. Wang, D. Xue, Z. Hu and X. Lu, *J. Biomed. Nanotechnol.*, 2018, **14**, 910–921.

110 M. M. Billingsley, N. Singh, P. Ravikumar, R. Zhang, C. H. June and M. J. Mitchell, *Nano Lett.*, 2020, **20**, 1578–1589.

111 Y. Zou, D. Mei, J. Yuan, J. Han, J. Xu, N. Sun, H. He, C. Yang and L. Zhao, *Int. J. Nanomed.*, 2021, **16**, 1127–1141.

112 Y. Yang, W. H. Zhao, W. W. Tan, Z. Q. Lai, D. Fang, L. Jiang, C. T. Zuo, N. Yang and Y. R. Lai, *Nanoscale Res. Lett.*, 2019, **14**.

113 S. Bi, S. Yue, W. Song and S. Zhang, *Chem. Commun.*, 2016, **52**, 12841–12844.

114 T. Suzawa, S. Nagamura, H. Saito, S. Ohta, N. Hanai, J. Kanazawa, M. Okabe and M. Yamasaki, *J. Contr. Release*, 2002, **79**, 229–242.

115 Y. L. Luo, Y. S. Shiao and Y. F. Huang, *ACS Nano*, 2011, **5**, 7796–7804.

116 Y. S. Youn and Y. H. Bae, *Adv. Drug Delivery Rev.*, 2018, **130**, 3–11.

117 S. Mondal, M. Saha, M. Ghosh, S. Santra, M. A. Khan, K. Das Saha and M. R. Molla, *Nanoscale Adv.*, 2019, **1**, 1571–1580.

118 H. Zhang, Y. Ma, Y. Xie, Y. An, Y. Huang, Z. Zhu and C. J. Yang, *Sci. Rep.*, 2015, **5**, 10099.

119 M. Liu, W. Ma, Q. Li, D. Zhao, X. Shao, Q. Huang, L. Hao and Y. Lin, *Cell Prolif.*, 2019, **52**.

120 Z. Fang, X. Wang, Y. Sun, R. Fan, Z. Liu, R. Guo and D. Xie, *Nanoscale*, 2019, **11**, 23000–23012.

121 C. Liu, J. Zheng, L. Deng, C. Ma, J. Li, Y. Li, S. Yang, J. Yang, J. Wang and R. Yang, *ACS Appl. Mater. Interfaces*, 2015, **7**, 11930–11938.

122 R. Ridolfo, B. C. Ede, P. Diamanti, P. B. White, A. W. Perriman, J. C. M. van Hest, A. Blair and D. S. Williams, *Small*, 2018, **14**, e1703774.

123 R. C. Deller, P. Diamanti, G. Morrison, J. Reilly, B. C. Ede, R. Richardson, K. Le Vay, A. M. Collins, A. Blair and A. W. Perriman, *Mol. Pharm.*, 2017, **14**, 722–732.

124 N. Dinauer, S. Balthasar, C. Weber, J. Kreuter, K. Langer and H. von Briesen, *Biomaterials*, 2005, **26**, 5898–5906.

125 N. Satake, J. Lee, K. Xiao, J. Luo, S. Sarangi, A. Chang, B. McLaughlin, P. Zhou, E. Kenney, L. Kraynov, S. Arnott, J. McGee, J. Nolta and K. Lam, *Proceedings of SPIE - the International Society for Optical Engineering*, Orlando, FL, 2011.

126 R. C. Huxford, K. E. Dekrafft, W. S. Boyle, D. Liu and W. Lin, *Chem. Sci.*, 2012, **3**, 198–204.

127 S. Habringer, C. Lapa, P. Herhaus, M. Schottelius, R. Istvanffy, K. Steiger, J. Slotta-Huspenina, A. Schirbel, H. Hanscheid, S. Kircher, A. K. Buck, K. Gotze, B. Vick, I. Jeremias, M. Schwaiger, C. Peschel, R. Oostendorp, H. J. Wester, G. U. Grigoleit and U. Keller, *Theranostics*, 2018, **8**, 369–383.

128 K. Wang, M. You, Y. Chen, D. Han, Z. Zhu, J. Huang, K. Williams, C. J. Yang and W. Tan, *Angew. Chem., Int. Ed.*, 2011, **50**, 6098–6101.

129 G. Yuan, M. Yao, H. Lv, X. Jia, J. Chen and J. Xue, *J. Med. Chem.*, 2020, **63**, 15655–15667.

130 H. Lu, W. Li, P. Qiu, X. Zhang, J. Qin, Y. Cai and X. Lu, *Nanoscale Adv.*, 2022, **4**, 4304–4313.

131 M. Harata, Y. Soda, K. Tani, J. Ooi, T. Takizawa, M. Chen, Y. Bai, K. Izawa, S. Kobayashi, A. Tomonari, F. Nagamura, S. Takahashi, K. Uchimaru, T. Iseki, T. Tsuji, T. A. Takahashi, K. Sugita, S. Nakazawa, A. Tojo, K. Maruyama and S. Asano, *Blood*, 2004, **104**, 1442–1449.

132 T. T. Smith, S. B. Stephan, H. F. Moffett, L. E. McKnight, W. Ji, D. Reiman, E. Bonagofski, M. E. Wohlfahrt, S. P. S. Pillai and M. T. Stephan, *Nat. Nanotechnol.*, 2017, **12**, 813–822.

133 V. Krishnan, X. Xu, D. Kelly, A. Snook, S. A. Waldman, R. W. Mason, X. Jia and A. K. Rajasekaran, *Mol. Pharm.*, 2015, **12**, 2101–2111.

134 Z. Lin, R. Peng, Y. Sun, L. Zhang and Z. Zhang, *Biosci. Rep.*, 2021, **41**.

135 V. Omelyanenko, P. Kopeckova, R. K. Prakash, C. D. Ebert and J. Kopecek, *Pharmaceut. Res.*, 1999, **16**, 1010–1019.



136 Y. Zhou, L. Guan, W. Li, R. Jia, L. Jia, Y. Zhang, X. Wen, S. Meng, D. Ma, N. Zhang, M. Ji, Y. Liu and C. Ji, *Cancer Lett.*, 2022, 533.

137 A. C. Martínez-Torres, D. G. Zarate-Triviño, H. Y. Lorenzo-Anota, A. Ávila-Ávila, C. Rodríguez-Abrego and C. Rodríguez-Padilla, *Int. J. Nanomed.*, 2018, 13, 3235–3250.

138 A. Szulc, L. Pulaski, D. Appelhans, B. Voit and B. Klajnert-Maculewicz, *Chem. Commun.*, 2016, 513, 572–583.

139 S. Harrach, C. Schmidt-Lauber, T. Pap, H. Pavenstädt, E. Schlatter, E. Schmidt, W. E. Berdel, U. Schulze, B. Edemir, S. Jeromin, T. Haferlach, G. Ciarimboli and J. Bertrand, *Blood Cancer J.*, 2016, 6, e470.

140 H. S. Rahman, A. Rasedee, A. B. Abdul, N. Allaудин, Zeenathul, H. H. Othman, S. K. Yeap, C. W. How, W. A. G. Wan and N. Hafiza, *Int. J. Nanomed.*, 2014, 9, 527–538.

141 S. M. Taghdisi, K. Abnous, F. Mosaffa and J. Behravan, *J. Drug Target.*, 2010, 18, 277–281.

142 Y. Liu, M. Lv, P. Bai, L. Wang, Y. Tan, H. Jian, R. Zhang, J. Zhu, S. Qu, S. Luo, L. Jiang, H. Nie, D. Guo, Z. Yu, Y. Li and W. Liang, *Int. J. Leg. Med.*, 2021, 135, 23–41.

143 H. Abbasi, N. Rahbar, M. Kouchak, P. Khalil Dezfuli and S. Handali, *J. Liposome Res.*, 2021, 1–16, DOI: [10.1080/08982104.2021.1903035](https://doi.org/10.1080/08982104.2021.1903035).

144 X. Wu, L. Wang, Y. Qiu, B. Zhang, Z. Hu and R. Jin, *Int. J. Nanomed.*, 2017, 12, 8025–8034.

145 F. M. Uckun, S. Qazi, I. Cely, K. Sahin, A. Shahidzadeh, I. Ozercan, Q. Yin, P. Gaynon, A. Termuhlen, J. Cheng and S. Yiv, *Blood*, 2013, 121, 4348–4354.

146 F. M. Uckun, D. E. Myers, J. Cheng and S. Qazi, *EBioMedicine*, 2015, 2, 554–562.

147 M. H. Amer, *Mol. Cell Ther.*, 2014, 2, 27.

148 D. Gan, Y. Chen, Z. Wu, L. Luo, S. K. Yirga, N. Zhang, F. Ye, H. Chen, J. Hu and Y. Chen, *Front. Pharmacol.*, 2021, 12.

149 Y. Y. Chen, D. H. Gan, L. P. Luo, Z. J. Wu, Y. W. Chen, H. J. Chen and J. D. Hu, *Blood*, 2020, 136.

150 C. Li, X. You, X. Xu, B. Wu, Y. Liu, T. Tong, J. Chen, Y. Li, C. Dai, Z. Ye, X. Tian, Y. Wei, Z. Hao, L. Jiang, J. Wu and M. Zhao, *Adv. Sci.*, 2022, e2104134.

151 T. A. Tabish, S. Zhang and P. G. Winyard, *Redox Biol.*, 2018, 15, 34–40.

152 B. Zhang, Y. Wang, J. Liu and G. Zhai, *Curr. Med. Chem.*, 2017, 24, 268–291.

153 B. P. Coughlin, P. T. Lawrence, I. R. Lui, C. J. Luby, D. J. Spencer, E. C. H. Sykes and C. R. Mace, *J. Nanopart. Res.*, 2020, 22(2), DOI: [10.1007/s11051-020-4765-1](https://doi.org/10.1007/s11051-020-4765-1).

154 Satrialdi, Y. Takano, E. Hirata, N. Ushijima, H. Harashima and Y. Yamada, *Nanoscale Adv.*, 2021, 3(20), 5919–5927.

155 L. Zou, H. Wang, B. He, L. Zeng, T. Tan, H. Cao, X. He, Z. Zhang, S. Guo and Y. Li, *Theranostics*, 2016, 6, 762–772.

156 J. Wang, M. You, G. Zhu, M. I. Shukoor, Z. Chen, Z. Zhao, M. B. Altman, Q. Yuan, Z. Zhu, Y. Chen, C. Z. Huang and W. Tan, *Small*, 2013, 9, 3678–3684.

157 L. F. Verdonck, H. M. Lokhorst, D. J. Roovers and H. G. van Heugten, *Leuk. Res.*, 1998, 22, 249–256.

158 R. R. Nair, D. Piktel, Q. A. Hathaway, S. L. Rellick, P. Thomas, P. Saralkar, K. H. Martin, W. J. Geldenhuys, J. M. Hollander and L. F. Gibson, *Pharm. Res.*, 2020, 37.

159 L. Warren, J. C. Jardillier, A. Malarska and M. G. Akeli, *Cancer Res.*, 1992, 52, 3241–3245.

160 B. C. Ede, P. Diamanti, D. S. Williams and A. Blair, *Sci. Rep.*, 2021, 11.

161 P. Tardi, S. Johnstone, N. Harasym, S. W. Xie, T. Harasym, N. Zisman, P. Harvie, D. Bermudes and L. Mayer, *Leuk. Res.*, 2009, 33, 129–139.

162 W. S. Lim, P. G. Tardi, X. Xie, M. Fan, R. Huang, T. Ciofani, T. O. Harasym and L. D. Mayer, *Leuk. Lymphoma*, 2010, 51, 1536–1542.

163 J. L. Millar, B. C. Millar, R. L. Powles, J. P. C. Steele, R. D. Clutterbuck, P. L. R. Mitchell, G. Cox, E. Forssen and D. Catovsky, *Br. J. Haematol.*, 1998, 102, 718–721.

164 M. M. Saber, A. M. Al-mahallawi and B. Stork, *Biomed. Pharmacother.*, 2021, 143.

165 Y. Zhang, M. Li, X. Gao, Y. Chen and T. Liu, *J. Hematol. Oncol.*, 2019, 12, 137.

166 M. Mazloum-Ardakani, B. Barazesh, A. Khoshroo, M. Moshtaghiun and M. H. Sheikhha, *Bioelectrochemistry*, 2018, 121, 38–45.

167 K. Y. Avelino, I. A. Frias, N. Lucena-Silva, R. G. Gomes, C. P. de Melo, M. D. Oliveira and C. A. Andrade, *Colloids Surf. B Biointerfaces*, 2016, 148, 576–584.

168 B. Greene, D. Alhatab, C. Pye and C. Brosseau, *J. Phys. Chem. C*, 2017, 121, 8084–8090.

169 J.-H. Kim, J.-S. Kim, H. Choi, S.-M. Lee, B.-H. Jun, K.-N. Yu, E. Kuk, Y.-K. Kim, D. H. Jeong and M.-H. Cho, *Anal. Chem.*, 2006, 78, 6967–6973.

170 W. Song, Z. Yan and K. Hu, *Biosens. Bioelectron.*, 2012, 38, 425–429.

171 S. Kainth and S. Basu, *Plasmonics*, 2018, 13, 1785–1793.

172 S. Zhang, L. Zhang, X. Zhang, P. Yang and J. Cai, *Analyst*, 2014, 139, 3629–3635.

173 N. S. Fracchiolla, S. Artuso and A. Cortelezzzi, *Sensors*, 2013, 13, 6423–6447.

174 Q. Liu, C. Jin, Y. Wang, X. Fang, X. Zhang, Z. Chen and W. Tan, *NPG Asia Mater.*, 2014, 6, e95.

175 M. Pirzada and Z. Altintas, *Sensors*, 2019, 19, 5311.

176 J. Yoon, M. Shin, T. Lee and J.-W. Choi, *Materials*, 2020, 13, 299.

177 S. M. Khoshfetrat and M. A. Mehrgardi, *Bioelectrochemistry*, 2017, 114, 24–32.

178 D. Shangguan, Z. C. Cao, Y. Li and W. Tan, *Clin. Chem.*, 2007, 53, 1153–1155.

179 G. Liu, X. Mao, J. A. Phillips, H. Xu, W. Tan and L. Zeng, *Anal. Chem.*, 2009, 81, 10013–10018.

180 G. G. Mironov, A. Bouzekri, J. Watson, O. Loboda, O. Ornatsky and M. V. Berezovski, *Anal. Bioanal. Chem.*, 2018, 410, 3047–3051.

181 Z. Yan, M. Yang, Z. Wang, F. Zhang, J. Xia, G. Shi, L. Xia, Y. Li, Y. Xia and L. Xia, *Sensor. Actuator. B Chem.*, 2015, 210, 248–253.

182 T. Zheng, T. Tan, Q. Zhang, J.-J. Fu, J.-J. Wu, K. Zhang, J.-J. Zhu and H. Wang, *Nanoscale*, 2013, 5, 10360–10368.



183 H. Kim, H. Terazono, M. Hayashi, H. Takei and K. Yasuda, *Jpn. J. Appl. Phys.*, 2012, **51**, 06FH01.

184 Y. Wu, K. Sefah, H. Liu, R. Wang and W. Tan, *Proc. Natl. Acad. Sci. U.S.A.*, 2010, **107**, 5–10.

185 Y. Pan, M. Guo, Z. Nie, Y. Huang, C. Pan, K. Zeng, Y. Zhang and S. Yao, *Biosens. Bioelectron.*, 2010, **25**, 1609–1614.

186 N. Naderian, M. Pourmadadi, H. Rashedi and F. Yazdian, Design of a Novel Nanobiosensor for the Diagnosis of Acute Lymphoid Leukemia (ALL) by Measurement of miRNA-128, in *2020 27th National and 5th International Iranian Conference on Biomedical Engineering (ICBME)*, 2020, IEEE, pp. 41–46.

187 M. El Aamri, G. Yammouri, H. Mohammadi, A. Amine and H. Korri-Youssoufi, *Biosensors*, 2020, **10**, 186.

188 Y. Yuan, Y. Wang, S. Liu, Y. Li, R. Duan, H. Zhang and X. Hu, *RSC Adv.*, 2016, **6**, 52255–52263.

189 W. Tang, W. Li, Y. Li, M. Zhang and X. Zeng, *New J. Chem.*, 2015, **39**, 8454–8460.

190 Z. Chen, G. Zhang, X. Chen, J. Chen, J. Liu and H. Yuan, *Biosens. Bioelectron.*, 2013, **41**, 844–847.

191 C. Maksoudian, N. Saffarzadeh, E. Hesemans, N. Dekoning, K. Buttiens and S. J. Soenen, *Nanoscale Adv.*, 2020, **2**, 3734–3763.

192 Y. D. Taghipour, R. Bahrami, A. M. Marques, R. Naseri, R. Rahimi, P. Haratipour, A. Iranpanah, A. I. Panah, M. H. Farzaei and M. Abdollahi, *Daru*, 2018, **26**, 229–239.

193 G. Brakmane, M. Winslet and A. M. Seifalian, *Aliment. Pharmacol. Ther.*, 2012, **36**, 213–221.

194 Z. Zhang, C. Tang, R. Hammink, F. H. T. Nelissen, H. A. Heus and P. H. J. Kouwer, *Chem. Commun.*, 2021, **57**, 2744–2747.

195 S. Li, L. Zhang, M. Li, J. Huang, B. Cui, J. Jia, Z. Guo, K. Ma and C. Cui, *J. Pharm. Sci.*, 2021, **110**, 2733–2742.

196 J. Ai, Y. Xu, D. Li, Z. Liu and E. Wang, *Talanta*, 2012, **101**, 32–37.

197 A. Tamashevski, Y. Harmaza, E. Slobozhanina, R. Viter and I. Iatsunskyi, *Molecules*, 2020, **25**, 3168.

198 A. Bahreyni, R. Yazdian-Robati, M. Ramezani, M. Rasouli, M. Alinezhad Nameghi, M. Alibolandi, K. Abnous and S. M. Taghdisi, *J. Biomater. Appl.*, 2017, **32**, 74–81.

199 M. Leitner, A. Poturnayova, C. Lamprecht, S. Weich, M. Snejdarkova, I. Karpisova, T. Hianik and A. Ebner, *Anal. Bioanal. Chem.*, 2017, **409**, 2767–2776.

200 Y. Yu, S. Duan, J. He, W. Liang, J. Su, J. Zhu, N. Hu, Y. Zhao and X. Lu, *Oncol. Rep.*, 2016, **36**, 886–892.

201 H. Li, H. Hu and D. Xu, *Anal. Chem.*, 2015, **87**, 3826–3833.

202 X. Pang, C. Cui, M. Su, Y. Wang, Q. Wei and W. Tan, *Nano Energy*, 2018, **46**, 101–109.

203 H. Yan, W. Ren, S. Liu and Y. Yu, *Anal. Chim. Acta*, 2020, **1106**, 199–206.

204 C. Chen, Y. Ho, S. Wu, G.-L. Chang and C. Lin, *J. Nanosci. Nanotechnol.*, 2009, **9**, 718–722.

